THE JOURNAL OF BIOLOGICAL CHEMISTRY
Vol. 279, No. 48, Issue of November 26, pp. 49795–49803, 2004
Printed in U.S.A.

Transcriptional Induction of *FosB*/Δ*FosB* Gene by Mechanical Stress in Osteoblasts*

Received for publication, April 13, 2004, and in revised form, September 13, 2004
Published, JBC Papers in Press, September 20, 2004, DOI 10.1074/jbc.M404096200

Daisuke Inoue‡, Shinsuke Kido, and Toshio Matsumoto

From the Department of Medicine and Bioregulatory Sciences, University of Tokushima Graduate School of Medicine, 3-18-15 Kuramoto-cho, Tokushima 770-8503, Japan

Mechanical stress to bone plays a critical role in maintaining bone mass and strength. However, the molecular mechanism of mechanical stress-induced bone formation is not fully understood. In the present study, we demonstrate that FosB and its spliced variant ΔFosB, which is known to increase bone mass by stimulating bone formation *in vivo*, is rapidly induced by mechanical loading in mouse hind limb bone *in vivo* and by fluid shear stress (FSS) in mouse calvarial osteoblasts *in vitro* both at the mRNA and protein levels. FSS induction of *FosB*/Δ*FosB* gene expression was dependent on gadlinium-sensitive Ca^{2+} influx and subsequent activation of ERK1/2. Analysis of the mouse *FosB*/Δ*FosB* gene upstream regulatory region with luciferase reporter gene assays revealed that the *FosB*/Δ*FosB* induction by FSS occurred at the transcriptional level and was conferred by a short fragment from −603 to −327. DNA precipitation assays and DNA decoy experiments indicated that ERK-dependent activation of CREB binding to a CRE/AP-1 like element (designated "CRE2") at the position of −413 largely contributed to the transcriptional effects of FSS. These results suggest that ΔFosB participates in mechanical stress-induced intracellular signaling cascades that activate the osteogenic program in osteoblasts.

Mechanical stress to bone plays a critical role in maintaining bone mass and strength. Reduced mechanical loading because of long-term bed rest or immobilization, or microgravity conditions in space, has been shown to cause significant bone loss and mineral changes. Evidence from human and animal studies has indicated that impaired bone formation significantly contributes to such unloading associated osteoporosis (1–3). Therefore, it is an important task for us to elucidate the mechanism by which mechanical loading induces bone formation to understand the pathophysiology and to establish an effective treatment of osteoporosis caused by reduced mechanical loading.

Bone cells have the ability to sense mechanical loading to activate multiple intracellular signaling pathways and transcription of various genes. Although the molecular device and the cellular repertoire in bone responsible for sensing such mechanical stimuli *in vivo* has not been precisely determined, it has been proposed that mechanotransduction in bone is mediated by changes in extracellular fluid flow caused by dynamic loading, which engenders fluid shear stress (FSS)[1] to bone cells, particularly osteocytes that are a terminally differentiated form of osteoblasts embedded in calcified bone (4, 5). Consistently, FSS has been shown to elicit a divergent array of intracellular signaling pathways including intracellular calcium rise, activation of enzymes such as protein kinase B/Akt, mitogen-activated protein kinase family, and activation of transcription factors such as AP-1 (activator protein-1) and CREB (cyclic AMP response element-binding protein) in cells of the osteoblast lineage (6–8). Downstream of such signaling events is induction of various gene expression including extracellular matrix proteins such as type I collagen and osteopontin, and growth factors such as insulin-like growth factor-I (7). However, the molecular mechanisms as well as relevance to bone formation of such gene induction by mechanical stress in bone cells are largely unknown.

One of the earliest transcriptional events caused by mechanical loading in bone cells is induction of *c-Fos* (9), a proto-oncogene that belongs to the AP-1 transcription factor family consisting of three Fos and four Jun family members. As a prototype of "immediate early genes," *c-Fos* expression is known to be rapidly and transiently induced by various stimuli including serum and growth factors (10–12). Induction of *c-Fos* expression by mechanical force has also been demonstrated in non-bone cells such as cardiac, muscle, and endothelial cells (13). Because mechanical loading induces several AP-1-responsive genes presumably involved in bone formation, *c-Fos* has been assumed to play a role in induction of such AP-1 target genes, thereby contributing to mechanical stress-induced bone formation. However, ubiquitous overexpression of *c-Fos* in transgenic mice resulted in development of osteosarcoma without evidence for increased bone formation (14). Therefore, although *c-Fos* may stimulate proliferation and/or survival of the osteoblast lineage cells, it is not able to induce bone formation when overexpressed alone in bone cells.

Another "immediate early gene" type member of the Fos family is FosB. Recently, transgenic mice overexpressing

* This work was supported by grants as part of the "Ground Research Announcement for Space Utilization" promoted by the Japan Science Forum (to T. M. and D. I.) and Grants-in-aid for Scientific Research on Priority Areas 12137207 (to T. M.) and Scientific Research (B) 14370329 (to T. M.) from the Ministry of Education, Science, Sports and Culture of Japan, and a Research fellowship of the Japan Society for the Promotion of Science for Young Scientists (to S. K.). The costs of publication of this article were defrayed in part by the payment of page charges. This article must therefore be hereby marked "*advertisement*" in accordance with 18 U.S.C. Section 1734 solely to indicate this fact.

The nucleotide sequence(s) reported in this paper has been submitted to the GenBank™/EBI Data Bank with accession number(s) AF093624.

‡ To whom correspondence should be addressed: Dept. of Medicine and Bioregulatory Sciences, University of Tokushima Graduate School of Medicine, 3-18-15 Kuramoto-cho, Tokushima 770-8503, Japan. Tel.: 81-88-633-9266; Fax: 81-88-633-7121; E-mail: inoued@clin.med.tokushima-u.ac.jp.

[1] The abbreviations used are: FSS, fluid shear stress; AP-1, activator protein-1; CREB, cyclic AMP response element-binding protein; ERK, extracellular signal-regulated kinase; COX, cyclooxygenase; SRE, serum response element; RT, reverse transcription; CDODN, circular dumbbell decoy oligonucleotides; BAPTA-AM, 1,2-bis(2-aminophenoxy)-ethane-*N*,*N*,*N*′,*N*′-tetraacetic acid, tetraacetoxymethyl ester; MEM, minimal essential medium.

ΔFosB (15–17), a short splicing isoform of *FosB* gene, have been reported to exhibit a progressive increase in bone mass because of enhanced bone formation (18). Expression of ΔFosB was observed within the osteoblast lineage and regulated in a differentiation-associated manner, and the effects of ΔFosB overexpression on osteoblasts appeared to be cell-autonomous and reversible (19, 20). These results indicate that expression of ΔFosB alone is sufficient to induce bone formation, and further imply that ΔFosB may be involved in signaling pathways induced by osteogenic stimuli such as mechanical loading.

In the present study, we investigated a potential role of ΔFosB in mechanical stress-induced bone formation. The results indicated that *FosB*/*ΔFosB* gene expression in bone cells was induced by mechanical stress both *in vitro* and *in vivo*. The induction occurred in a manner dependent on gadolinium (Gd^{3+})-sensitive Ca^{2+} influx and ERK (extracellular signal-regulated kinase) but independent of prostaglandin production, and involved a transcriptional mechanism with a major contribution of CREB. Our results suggest that ΔFosB acts as a downstream effector of mechanical loading and participates in mechanical stress-induced osteogenic signaling pathways.

EXPERIMENTAL PROCEDURES

Materials—A selective cyclooxygenase (COX)-2 inhibitor, JTE-522 (21, 22), was a kind gift from Japan Tobacco Inc. (Osaka, Japan). Indomethacin, nifedipine (L-type Ca^{2+} channel blocker), BAPTA-AM (intracellular Ca^{2+} chelator), A23187 (calcium ionophore), bucladesine (dibutyryl cAMP), U0126 (ERK inhibitor), and SB203580 (p38 kinase inhibitor) were purchased from Calbiochem. pAP1-Luc, pCRE-Luc, and pSRE-Luc plasmids, which are *cis*-reporter plasmids containing tandem consensus AP-1-binding sites, CRE (cAMP-response element), and *c-Fos*-derived SRE (serum response element), respectively, were from Invitrogen. All chemicals for dual-luciferase reporter assays were from Promega (Madison, WI). Antibody against FosB/ΔFosB was from Santa Cruz Biotechnology (San Diego, CA). Polyclonal antibodies against ERK1/2 and activated (phospho-) ERK1/2 were from Promega, and anti-CREB and phospho-CREB antibodies were from New England Biolabs (Beverly, MA). All DNA modifying enzymes used in this study were from New England Biolabs Inc. and the other reagents were from Sigma unless otherwise indicated.

Experimental Animals—For *in vivo* experiments, 7–9-week-old ICR male mice were purchased from Charles River Japan (Tokyo, Japan), and were acclimatized for 1 week. The body weight of the mice ranged from 20 to 25 g. All mice were allowed free access to food and water, housed in stainless cages in an air-conditioned environment (temperature: 24–25 °C, humidity: 50–55%) that was illuminated from 8:00 a.m. to 8:00 p.m. The experimental protocols in the current study have been approved by the Institutional Animal Care and Oversight Committee according to the guideline principles in the Care and Use of Animals. Mechanical unloading by tail suspension and the following reloading was performed according to the procedures described before (23, 24) with slight modifications. Mice were anesthetized with ether and unloaded by suspending tails with the hind limbs being lifted off from the ground. After tail suspension for 4 days, mice were forced to run in rotating cages for the indicated times for reloading, sacrificed, and analyzed for gene expression.

Cell Culture—Primary osteoblasts were prepared from calvariae of newborn ICR mice by sequential digestion with 0.1% (w/v) type IA collagenase and 0.2% (w/v) dispase as previously described (25). The osteoblasts were cultured in α-MEM supplemented with 10% fetal bovine serum (fetal bovine serum) (Sigma), penicillin/streptomycin (Invitrogen) for 48 h. Before induction experiments, 1×10^5/ml osteoblasts were plated on culture dishes, grown to 70–80% confluence, and serum-deprived in α-MEM with 1% fetal bovine serum for 24 h. For mechanical loading *in vitro*, osteoblasts were exposed to FSS by placing 6-well culture dishes on a horizontal shaking apparatus fixed inside the culture incubator. All the experiments in the present study were performed at 100–120 rpm. The shear stress force in our system was estimated to be slightly less than that produced by 200 rpm with a cone viscometer, which was ~2 pascal at the edge (26), and thus theoretically stayed within the physiological range.

Adenovirus Infection—A recombinant adenoviral vector for constitutively active MEK1 (MEK^{CA}) was a kind gift from Dr. Sakae Tanaka (University of Tokyo). Primary osteoblasts at passage two were infected with MEK^{CA} adenoviruses at a multiplicity of infection varying from 0 to 100. At 48 h after infection, cells were harvested and examined for expression of FosB/ΔFosB and other proteins by Western blot analysis.

RNA Analysis—Total RNA was extracted from tibia and femur of the mice or cultured primary osteoblasts using TRIzol reagents (Invitrogen), and mRNA expression for various genes was determined by reverse transcription-polymerase chain reaction (RT-PCR) or ribonuclease (RNase) protection assays. For RT-PCR, 1 μg of total RNA was reverse-transcribed using SuperScript II RT™ (Invitrogen) and random primers (Promega Corp., Madison, WI). One of a 20-μl RT reaction was used for PCR analysis. Primer sets used for amplification were as follows: sense, 5′-aaaaggcagagctggagtcgg-3′, and antisense, 5′-tgtacgaagggctaacaacgg-3′ for mouse FosB, which amplifies both the short spliced Δ*FosB* isoform and the long *FosB* transcripts; and sense, 5′-tgtcttcaccaccatggagaagg-3′, and antisense, 5′-gtggatgcagggatgatgttctg-3′, for mouse GAPDH gene. The PCR cycle numbers were 28 for *FosB*/Δ*FosB* and 22 for GAPDH, which were determined so that quantitative information was not lost. Amplified products were separated on 1.5–2.0% agarose gels and stained with ethidium bromide for visualization. For the RNase protection assay, a fragment of mouse FosB cDNA (nucleotides 1480–2051) was subcloned into pBlueScript SKII(+) (Stratagene, La Jolla, CA). The resultant plasmid was linearized and purified with Gel Extraction Kit (Qiagen Inc., Valencia, CA) and *in vitro* transcribed to generate a cRNA probe using the MAXIscript *in Vitro* Transcription Kit (Ambion Inc., Austin, TX). A control template for mouse β-actin was purchased from Ambion. RNase protection assays were performed using the RPAII Kit (Ambion) as previously described (27). Briefly, RNA samples were incubated with [α-^{32}P]UTP-labeled cRNA probes at 42 °C for 18 h and digested with an RNase A/T1 mixture. Non-digested RNA was precipitated, separated on a 6% polyacrylamide gel containing 8 M urea, transferred to 3MM Whatman filter paper, dried, and autoradiographed.

Protein Analysis—Preparation of nuclear extracts was described previously (25). Briefly, 1–2 × 10^7 cells were collected, washed twice with ice-cold phosphate-buffered saline, incubated in ice-cold hypotonic buffer (10 mM HEPES-KOH, pH 7.2, 10 mM KCl, 0.1 mM EDTA, 0.1 mM EGTA, 0.75 mM spermidine, 0.15 mM spermine, 1 mM dithiothreitol, 0.5 mM phenylmethylsulfonyl fluoride, 1× protease inhibitor mixture (Sigma), and 10 mM Na_2MoO_4) for 10 min, vortexed for 10 s, and centrifuged at 15,000 × *g* at 4 °C for 60 s. The pellet was resuspended in NLB buffer (20 mM HEPES-KOH, pH 7.2, 0.4 M NaCl, 1 mM EDTA, 1 mM EGTA, 1 mM dithiothreitol, 0.5 mM phenylmethylsulfonyl fluoride, 1× Protease inhibitor mixture (Sigma), and 10 mM Na_2MoO_4), placed on ice for 15 min, and centrifuged at 4 °C at 15,000 × *g* for 10 min. The supernatant was saved as nuclear extracts. Total cell lysates were prepared using 1× Cell Lysis Buffer (Cell Signaling Technology Inc., Beverly, MA) according to the manufacturer's instructions. The nuclear extracts and total cell lysates were stored at −80 °C until use. For Western blot analysis, 30 μg of protein was separated on a 5–20% gradient SDS-PAGE and transferred to polyvinylidene difluoride membrane (Millipore Corp.). The membrane was rinsed and blocked with 5% nonfat skim milk or 2% bovine serum albumin (fraction V from Sigma) in Tris-buffered saline (TBS) with 0.1% Tween 20 for 2 h at room temperature, blotted sequentially with primary antibodies, then with a horseradish-conjugated secondary antibody for 1 h, and the protein bands were visualized with an ECL detection system (Amersham Biosciences).

Cloning of the Mouse FosB Gene Promoter—Fragments of mouse *FosB* gene (GenBank™ number AF093624) upstream regulatory region from nucleotides −1000 to +307 (1.0K), −603 to +307 (0.6K), and −327 to +307 (0.3K) (with the transcription start site being numbered +1) were cloned from a mouse genomic library (Toyobo Co., Ltd., Osaka, Japan) by PCR with the following primer sets: sense, 5′-acgggtacct-tagtctccggttcggagaaac-3′, and antisense, 5′-acgaagcttttagtctccggttcg-gagaaac-3′, for 1.0K; sense, 5′-ctaattgcgtcacaggaactcc-3′, and antisense, acgaagcttttagtctccggttcggagaaac-3′ for 0.6K; and sense, 5′-agcggtac-ccagggtcacactatgggcaggt-3′, and antisense, 5′-acgaagcttttagtctccggttcg-gagaaa-3′, for 0.3K. PCR products were purified, digested with KpnI/XhoI (1.0K and 0.3K) or SmaI/XhoI (0.6K), and subcloned into a luciferase reporter plasmid pGL3-basic (Promega, Madison, WI), which lacks eukaryotic promoter and enhancer sequences. From the luciferase vector containing the longest 1.0-kb promoter, a series of mutant plasmids were generated by site-directed mutagenesis using the QuikChange™ Site-directed Mutagenesis Kit (STRATAGENE) with mutagenic primers including 5′-ccttatatCC-3′ for SRE mutation (g547c and g548c) and 5′-tgGCAca-3′ for CRE2 mutation (c556g, g557c, and t558a). All the constructs were verified by sequencing.

Dual Luciferase Assay—Osteoblasts were seeded in 6-well culture

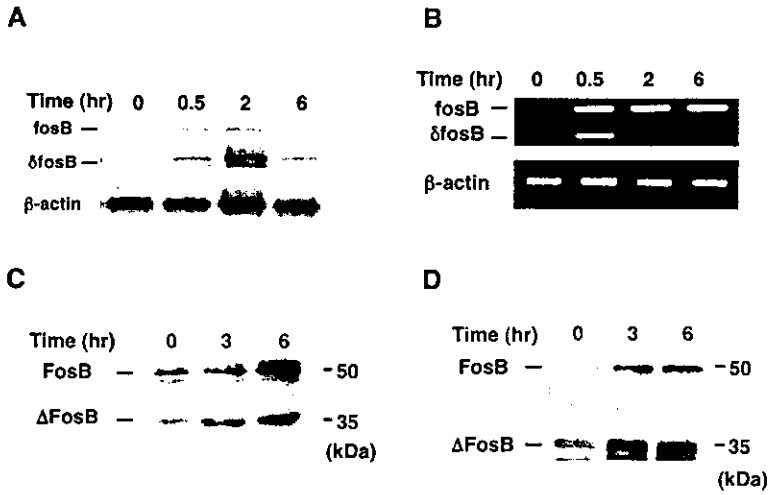

FIG. 1. ***In vivo* and *in vitro* induction of *FosB/ΔFosB* gene expression at mRNA and protein levels by mechanical stress in bone cells.** For *in vivo* experiments (*A* and *C*), 7–9-week-old ICR male mice were tail suspended for 4 days and were reloaded in a rotating cage for the indicated times. Mice were sacrificed, and total RNA and total cell lysate was extracted from tibiae and femurs and analyzed for mRNA (*A*) and protein (*C*) expression of *FosB/ΔFosB* gene by RNase protection assay and Western blot analysis, respectively. *In vitro* experiments were performed by culturing mouse calvarial osteoblasts for 48 h and then exposing them to FSS for the indicated times. Expression of *FosB/ΔFosB* gene expression was analyzed at both mRNA (*B*) and protein (*D*) levels by RT-PCR and Western blot analysis, respectively.

plates at 50% confluence and cultured in α-MEM supplemented with 10% fetal bovine serum. After 18–24 h, the cells were co-transfected with 1 μg of chimeric luciferase reporter plasmids and 0.025 μg of pRL-TK Renilla luciferase plasmids (Promega) using GenePorter 2 Transfection Reagents (Gene Therapy Systems, Inc., San Diego, CA) in Opti-MEM supplemented with 1% fetal bovine serum. At 6 h after transfection, the medium was replaced by 2 ml of Opti-MEM supplemented with 1% fetal bovine serum, and the cells were incubated for an additional 24 h. The transfected cells were then treated with various reagents and/or exposed to FSS by placing the culture plates on a shaking apparatus at 100 to 120 rpm. For dual luciferase assays, the cells were washed twice with PBS and lysed with 100 μl of passive cell lysis buffer (Promega). Luciferase activities were measured with luminometer (ATTO, Tokyo, Japan) by mixing 50 μl of luciferase substrate solution (Promega) with 10 μl of cell lysates. Transcriptional activity was normalized for Renilla luciferase activity or protein concentrations.

Electrophoretic Mobility Shift Assay—Electrophoretic mobility shift assay was performed as previously described (25). Radiolabeled double-stranded oligonucleotide probes were prepared by annealing complementary oligonucleotides end-labeled with [α-^{32}P]dATP and DNA polymerase I fragment (Klenow) (New England Biolabs). The labeled probes were purified by Sephadex G-25 columns (Quick Spin Columns, Roche Molecular Biochemicals), diluted with distilled water, and 3 × 10^4 cpm was incubated with nuclear extracts (10 μg) and 4 μg of poly(dI-dC)·poly(dI-dC) in a total volume of 20 μl of 1/2 × NLB buffer at 4 °C for 30 min. For competition analysis, a hundred times molar excess of cold oligonucleotide probes were added to the electrophoretic mobility shift assay reaction. Resolution was accomplished by electrophoresing 15 μl of the reaction mixture on 4.5 to 5.0% polyacrylamide gels using 0.25× TBE buffer (22.3 mM Tris-HCl, 22.3 mM boric acid, and 0.25 mM EDTA, pH 8.0). Gels were then transferred onto 3MM filter paper and dried, and protein-DNA complexes were visualized by autoradiography.

DNA Precipitation Assay—Biotinylated double-stranded oligonucleotide probes containing three tandem repeats of SRE/CRE2 (−437 to −401) or CRE1 (−488 to −461) sequences were prepared by annealing complementary oligonucleotides followed by ethanol precipitation. The annealed probes (100 pmol) were incubated with 100 μg of nuclear extracts and 15 μg of poly(dI-dC)·poly(dI-dC) in 500 μl of NLB100 buffer (20 mM HEPES-KOH, pH 7.2, 0.1 M NaCl, 1 mM EDTA, 1 mM EGTA, 0.5 mM dithiothreitol, 1 mM phenylmethylsulfonyl fluoride, protease inhibitor mixture (Sigma), 20 mM sodium fluoride, and 1 mM VO_4 for 4 °C with gentle agitation, and then with streptavidine-conjugated magnetic beads (Magnotex-SA, TaKaRa, Japan) at 4 °C for 30 min. DNA-protein complexes bound to magnetic beads were collected by placing the reaction tubes on a magnetic stand and washed with ice-cold NLB100 buffer for four times. After the final wash, beads were collected and resuspended in 2× sample buffer. Sequence-specific DNA-bound proteins were separated on a SDS-polyacrylamide gel and detected by Western blotting. For competition analysis, 100 times molar excess of non-labeled biotinylated double-stranded oligonucleotide probes were added to the DNA-protein reactions.

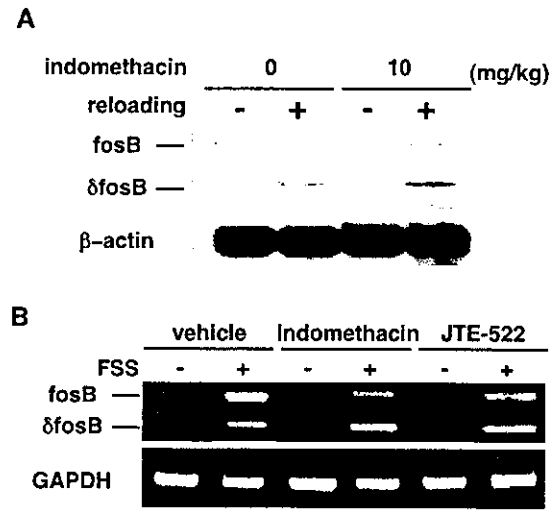

FIG. 2. **Induction of *FosB/ΔFosB* mRNA is independent of prostaglandin production.** *A*, 7–9-week-old ICR male mice were first tail suspended for 4 days and orally given 10 mg/kg of indomethacin or vehicle. After 1 h, mice were reloaded in a rotating cage for 30 min and sacrificed, and expression of *FosB/ΔFosB* and β-actin mRNA in tibiae and femurs was analyzed by RNase protection assay. *B*, mouse calvarial osteoblasts were pretreated with 1 mM indomethacin or a selective COX-2 inhibitor, JTE-522, 30 min prior to FSS. Cells were then exposed to FSS for 30 min, and mRNA expression of *FosB/ΔFosB* and GAPDH as an internal control was examined by RT-PCR.

Decoy Oligonucleotides—An SRE/CRE2 "circular dumbbell" decoy oligonucleotide (CDODN) (28, 29) containing the SRE/CRE2 sequences in the *FosB* promoter region (5′-ataaggagctcgccttttttggcgagctccttatatggctaattgcgtcacaggttttttcctgtgacgcaattagccat-3′) was synthesized to form a double-stranded DNA oligomer with the both ends hinged by a stretch of seven Ts. This structure has been demonstrated to confer resistance to endogenous nucleases (29). As controls, we also synthesized mutant CDODNs including: Scramble, 5′-taacgactcggtagttttttctaccgagtcgttaattgcctgcggcagtggatgttttttcatccactgccgcaggcaat-3′; SREmt, 5′-ataaCCagctcgccttttttggcgagctGGttatatggctaattgcgtcacaggttttttcctgtgacgcaattagccat-3′; and CRE2mt, 5′-ataaggagctcgccttttttggcgagctccttatatggctaattgGCAcacaggttttttcctgtgTGCcaattagccat-3′. After self-annealing and ligation, the CDODNs

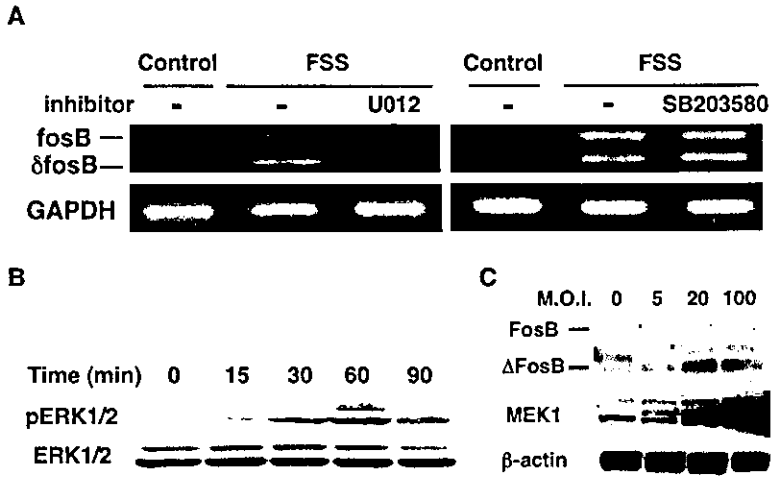

FIG. 3. **FSS-induced *FosB/ΔFosB* induction is dependent on ERK.** *A*, primary calvarial osteoblasts were pretreated with 10 μM U0126, 10 μM SB203580, or a vehicle for 30 min. Cells were then exposed to FSS for 30 min and analyzed for *FosB/ΔFosB* and GAPDH mRNA expression by RT-PCR. *Control* is a negative control without FSS. *B*, to evaluate ERK activation by FSS, cells were exposed to FSS for the indicated times, lysed, and examined by Western blot analysis using antibodies against phosphorylated (pERK1/2) and total ERK1/2. *C*, primary osteoblasts were infected with an adenovirus expressing constitutively active MEK1 (MEK^{CA}) (44) at increasing multiplicity of infection for 48 h, and analyzed for FosB/ΔFosB, MEK1, and β-actin expression by Western blotting.

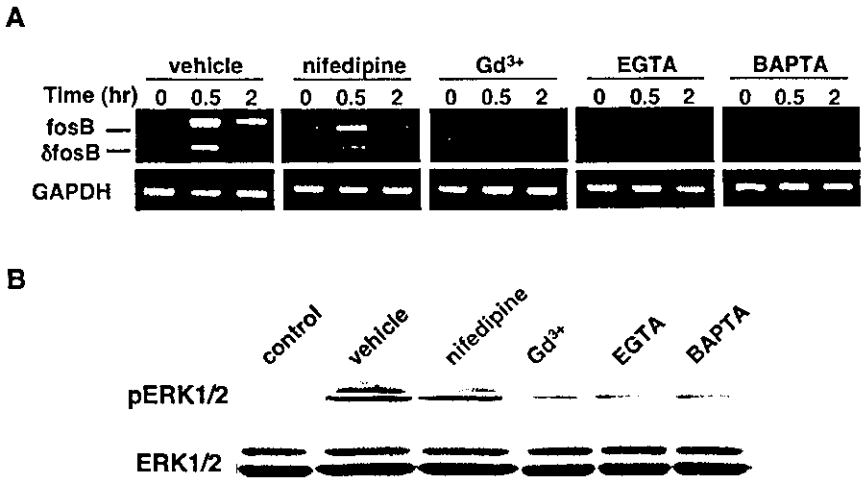

FIG. 4. **FSS-induced *FosB/ΔFosB* induction was dependent on Ca^{2+} influx through a Gd^{3+}-sensitive cation channel.** Mouse calvarial osteoblasts were pretreated with vehicles, 10 μM nifedipine, 10 μM gadolinium chloride (Gd^{3+}), 2.5 mM EGTA, or 50 μM BAPTA-AM for 30 min and then exposed to FSS for 30 min. Levels of *FosB/ΔFosB* and GAPDH mRNA expression and ERK phosphorylation were determined by RT-PCR (*A*) and Western blot analysis, respectively (*B*).

were introduced into osteoblasts by GenePorter 2 Transfection Reagents according to the manufacturer's instruction.

RESULTS

In Vivo Mechanical Forces and in Vitro FSS to Osteoblasts Induce FosB/ΔFosB Gene Expression at Both the mRNA and Protein Levels—We first investigated whether or not expression of the *FosB/ΔFosB* gene in bone is induced by mechanical loading *in vivo*. Seven- to 9-week-old ICR male mice were tail suspended for 4 days to reduce the background expression, and then mechanically reloaded in rotating cages. As shown in Fig. 1*A*, expression of (long) *FosB* and *ΔFosB* mRNA in tibiae and femurs was undetectable in tail-suspended mice, but was induced as early as 30 min after mechanical reloading and reached the maximum within 2 h. In the *in vitro* experiments shown in Fig. 1*B*, primary osteoblasts derived from newborn mouse calvariae were subjected to FSS on a shaking apparatus. As a result, we observed that *FosB/ΔFosB* mRNA was induced by FSS in primary osteoblasts, recapitulating the *in vivo* induction in reloaded mice. These results are consistent with an assumption that the *in vivo* mechanical forces caused FSS to bone cells of the osteoblast lineage, leading to increased expression of FosB/ΔFosB. To confirm that the induction of *FosB/ΔFosB* mRNA by FSS leads to an increase in the amount of their protein products, nuclear extracts were obtained from cells that had been exposed to FSS and were analyzed for FosB/ΔFosB protein expression by Western blotting. The results indicated that FosB (50 kDa) and ΔFosB (32 kDa) proteins were both induced either by mechanical loading *in vivo* or FSS *in vitro* in a time-dependent manner (Fig. 1, *C* and *D*). These findings were similarly observed in other osteoblastic cell lines such as a murine calvarial cell line, MC3T3-E1, and a murine bone marrow stromal cell line, ST-2 (data not shown). Therefore, induction of *FosB/ΔFosB* gene expression by mechanical stress occurs at both the mRNA and protein levels in cells of the osteoblast lineage.

Induction of FosB/ΔFosB mRNA Is Independent of Prostaglandin Production—Previous reports suggest that prostaglandins are important mediators of mechanical stress-induced bone formation. Mechanical stress has been shown to cause activation of a constitutive type of prostaglandin G/H synthase (COX-1) and transcriptional up-regulation of an inducible isoform (COX-2) (8, 30), and both events would lead to increased production of prostaglandins, especially the E series that have been shown to induce *c-Fos* (31). To determine whether FSS-induced *FosB/ΔFosB* expression is mediated by prostaglandins, tail-suspended mice were subcutaneously injected with indo-

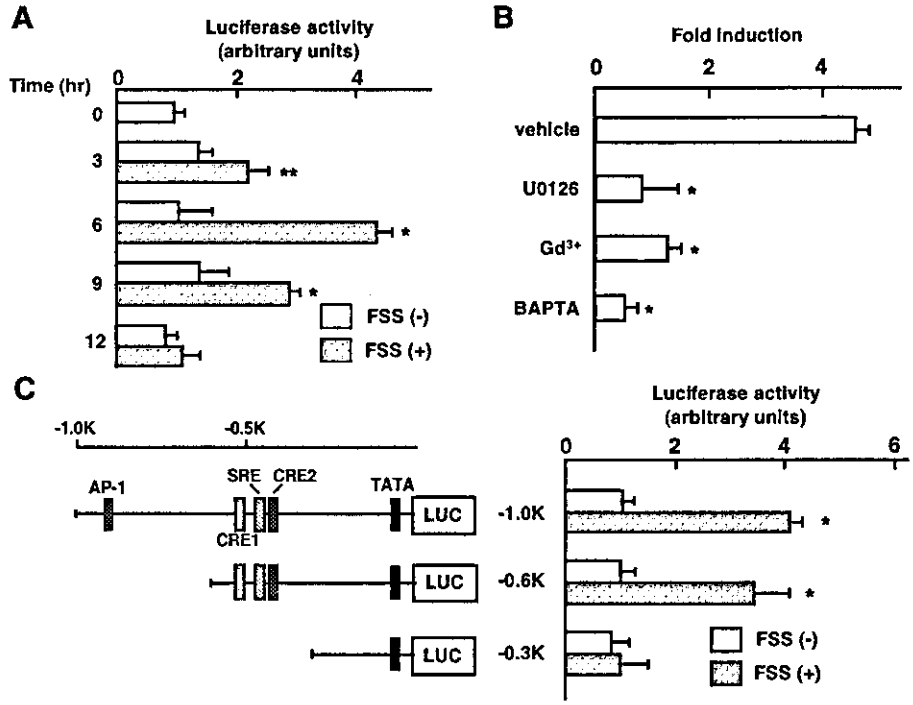

FIG. 5. **Induction of *FosB/ΔFosB* gene transcription by FSS occurs through a short region containing SRE and two CREs in a manner dependent on Ca^{2+} and ERK.** *A*, a chimeric luciferase reporter plasmid including the 5′-flanking region of the mouse *FosB/ΔFosB* gene (*1.0K*) was transiently transfected into primary osteoblasts. Cells were then exposed to FSS for the indicated times and transcriptional activity was measured by dual-luciferase assay. Data were corrected for Renilla luciferase and expressed as a mean of four independent experiments with an error bar of S.D. in arbitrary units. **, significantly different ($p < 0.05$) from FSS (−). *, significantly different ($p < 0.01$) from FSS (−). *B*, osteoblasts transfected with the *FosB/ΔFosB* gene promoter construct (*−1.0K*) were exposed to FSS in the presence of vehicle, 10 μM U0126, 10 μM gadolinium chloride, or 50 μM BAPTA-AM for 6 h, and transcriptional activity was measured by dual luciferase assay. Data were expressed as a mean of four independent experiments with an error bar of S.D. in -fold induction by FSS. *, significantly different ($p < 0.01$) from the vehicle control. *C*, various deletion constructs (*−1.0K*, *−0.6K*, and *−0.3K*) were transfected into primary osteoblasts, and analyzed for transcriptional response to FSS. Potential transcription factor binding sites are shown. Data were corrected for Renilla luciferase and expressed as a mean of four independent experiments with an error bar of S.D. in arbitrary units. *, significantly different ($p < 0.01$) from FSS (−).

methacin, a general COX inhibitor (both COX-1 and COX-2), prior to reloading, and *FosB/ΔFosB* mRNA induction in tibiae and femurs was analyzed by RNase protection assay. As shown in Fig. 2*A*, *FosB/ΔFosB* mRNA induction was not blocked by indomethacin. Similarly, pretreatment with either indomethacin or a selective COX-2 inhibitor, JTE-522, had no major effects on FSS-induced *FosB/ΔFosB* expression in osteoblasts *in vitro* (Fig. 2*B*). These results indicated that mechanical stress-induced *FosB/ΔFosB* induction was independent of prostaglandin production both *in vivo* and *in vitro*.

FSS-induced FosB/ΔFosB mRNA Expression Is Dependent on ERK—We then attempted to delineate the intracellular signaling pathways leading to FosB/ΔFosB induction. We first investigated involvement of the mitogen-activated protein kinase family members including ERK, p38 kinase, and c-Jun N-terminal kinase, which have been suggested to link FSS to various gene inductions (32, 33). Primary osteoblasts were exposed to an ERK1/2 inhibitor, U0126, or p38 kinase inhibitor, SB203580, and then subjected to FSS. As shown in Fig. 3*A*, U0126, as well as another ERK inhibitor PD98059 (data not shown), completely abolished *FosB/ΔFosB* mRNA induction, whereas SB203580 had no effects. Consistent with a critical role of ERK, we found that FSS activated ERK1/2 as early as 15 min as shown by Western blot analysis using an anti-phosphorylated ERK1/2 antibody (Fig. 3*B*). Moreover, activation of ERK1/2 by adenoviral overexpression of constitutively active MEK1 resulted in up-regulation of FosB/ΔFosB protein expression in a dose-dependent manner (Fig. 3*C*). In our *in vitro* system, we observed little if any activation of other mitogen-activated protein kinase family members such as p38 kinase and c-Jun N-terminal kinase in response to FSS (data not shown). These results indicated that FSS induction of *FosB/ΔFosB* mRNA expression was dependent on ERK.

ERK-mediated FosB/ΔFosB Induction by FSS Is Dependent on Gd^{3+}-sensitive Ca^{2+} Influx—Evidence suggests that mechanical stress to bone causes a rapid rise in intracellular Ca^{2+} concentration in bone-forming cells, one of the earliest events that initiate divergent downstream signaling cascades in response to mechanical stress (6–8). However, the channel responsible for the mechanical stress-induced Ca^{2+} influx leading to bone formation *in vivo* has not been precisely determined, and the types and features of the channels thus far reported are considerably variable depending upon the *in vitro* experimental system and the output for evaluation. Accordingly, several types of Ca^{2+} channels have been implicated in the mechanical stress-induced signaling pathways, particularly L-type voltage-dependent Ca^{2+} channel, and a hypothetical mechanosensitive cation channel that is blocked by gadlinium ions (Gd^{3+}) (6). We therefore tested effects of various inhibitors of Ca^{2+} signaling on *FosB/ΔFosB* induction by FSS. As shown in Fig. 4*A*, *FosB/ΔFosB* induction was completely blocked by extracellular (EGTA) and intracellular (BAPTA-AM) Ca^{2+} chelators, and Gd^{3+}, suggesting involvement of a Gd^{3+}-sensitive Ca^{2+} channel. Neither voltage-dependent Ca^{2+} channel inhibitors, nifedipine (Fig. 4*A*) nor verapamil (data not shown), affected the *FosB/ΔFosB* mRNA induction. We examined the same set of inhibitors for the effects on FSS-induced ERK activation, and obtained virtually the same results (Fig. 4*B*). We also confirmed that Ca^{2+} ionophores such as A23187 and ionomycin induced both ERK activation and *FosB/ΔFosB*

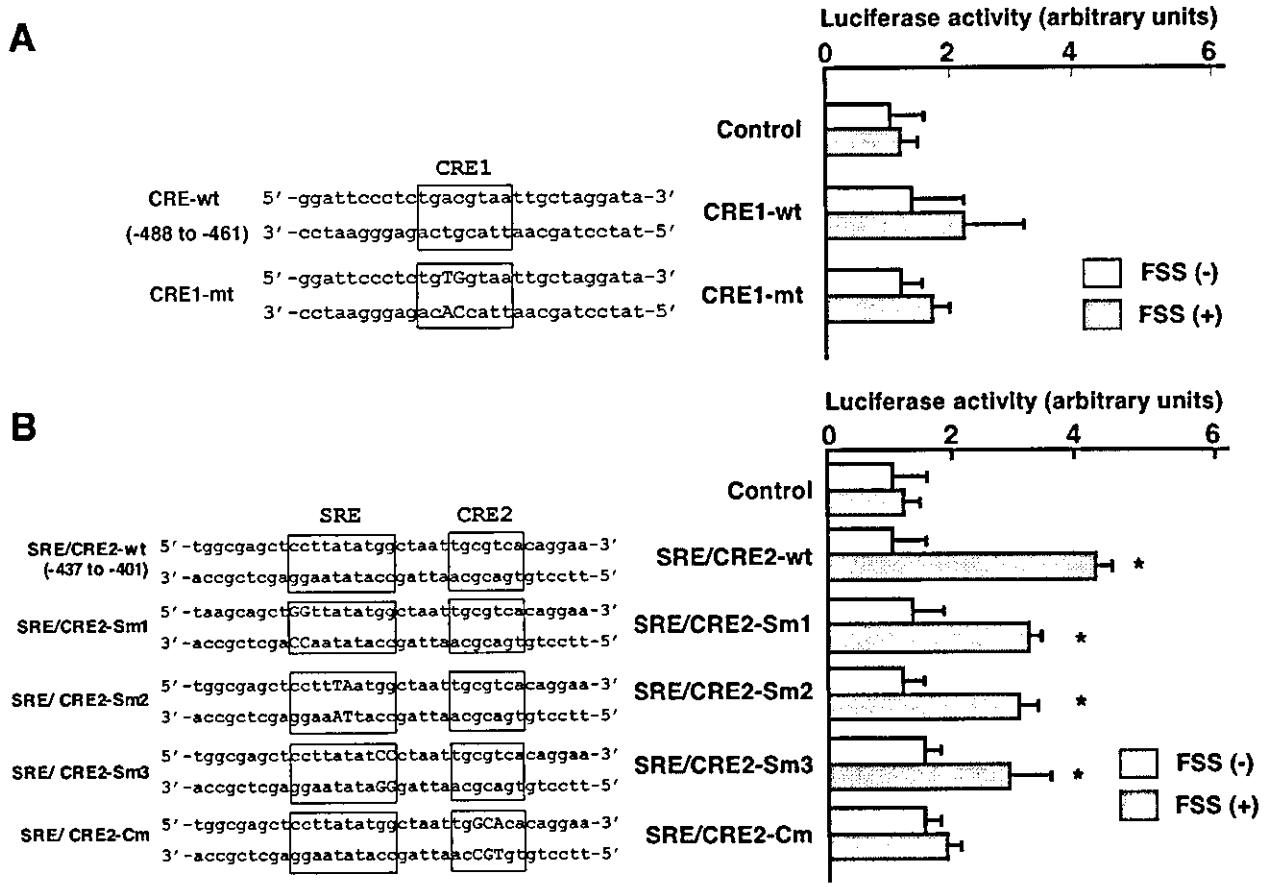

FIG. 6. **Sequences corresponding to CRE2, but not CRE1 or SRE, confer the transcriptional response of the *FosB* gene to FSS.** Oligonucleotides corresponding to potential FSS response elements in the *FosB* promoter and their mutants (*A*, CRE1, upstream CRE-like sequences; *B*, SRE/CRE2, serum response element like-sequences and downstream CRE-like sequences) were subcloned into a luciferase vector in 3× tandem, and tested for a transcriptional response to FSS. Substituted nucleotides are shown as *bold*. Data were corrected for Renilla luciferase and expressed as a mean of four independent experiments with an error bar of S.D. in arbitrary units. *, significantly different ($p < 0.01$) from FSS (−).

mRNA expression in osteoblasts (data not shown). Taken together, these results suggested that FSS induced *FosB*/*ΔFosB* mRNA expression in a manner dependent on Ca^{2+} influx through a Gd^{3+}-sensitive cation channel and the subsequent ERK activation.

Induction of FosB/ΔFosB Expression by FSS Occurs at the Transcriptional Level—To determine whether induction of *FosB*/*ΔFosB* mRNA expression by FSS occurred at the transcriptional level, we cloned and analyzed the mouse *FosB*/*ΔFosB* gene promoter (34). A genomic fragment (−1000 to +307) containing a TATA box and a 1.0-kb long upstream regulatory region of the *FosB* gene was obtained by genomic polymerase chain reaction and subcloned into a luciferase reporter vector PGL3-basic. The resultant vector pGL3–1.0K was transfected into primary osteoblasts, and the promoter activities were measured in the absence or presence of FSS *in vitro*. As shown in Fig. 5*A*, FSS stimulated *FosB* gene promoter activity in a time-dependent manner, with a peak being ~4-fold induction at 6 h. Consistent with the results of mRNA expression studies shown in Figs. 3 and 4, the induction was almost completely abrogated by an ERK inhibitor U0126, Gd^{3+}, or an intracellular Ca^{2+} chelator BAPTA-AM (Fig. 5*B*). Thus, FSS induced *FosB*/*ΔFosB* gene transcription in a manner dependent on a Gd^{3+}-sensitive cation channel and ERK.

Cyclic AMP Response Element-like Sequences (CRE2) Contribute to FSS-induced FosB/ΔFosB Gene Transcription—We then attempted to determine DNA elements mediating FSS-induced *FosB*/*ΔFosB* gene transcription. For this purpose, we first generated two deletion constructs, PGL-0.6K containing a promoter fragment from −603 to +307 and PGL-0.3K containing a fragment from −327 to +307, and tested FSS effects on promoter activities of these two deletion constructs together with the original PGL-1.0K containing a region between −1,000 and +327. As shown in Fig. 5*C*, the response was retained in PGL-0.6K but significant induction by FSS was lost in PGL-0.3K, indicating that the transcriptional response to FSS was conferred by a region between −603 and −327.

It has been suggested that *FosB* and *c-Fos* genes have evolved from a common ancestor gene by gene duplication (34). Accordingly, these genes have a similar genomic organization and are subject to a similar mode of transcriptional regulation as an immediate early gene, and most of the critical DNA elements in the *c-Fos* gene promoter are also conserved in the upstream regulatory region of the *FosB* gene (11, 12). We found that such key elements were present in the *FosB*/*ΔFosB* promoter region between −607 and −327 that we have identified to confer the shear stress response: an upstream CRE or AP-1 like sequences from −479 to −470 that we designated CRE1, and SRE from −428 to −419 with an immediately downstream CRE or AP-1 from −413 to −407 (we designated SRE/CRE2) (Fig. 5*C*). We therefore examined whether each of these elements, whose counterparts in the *c-Fos* gene have been shown to play an important role in its transcriptional regulation, were able to respond to FSS. When an oligonucleotide corresponding

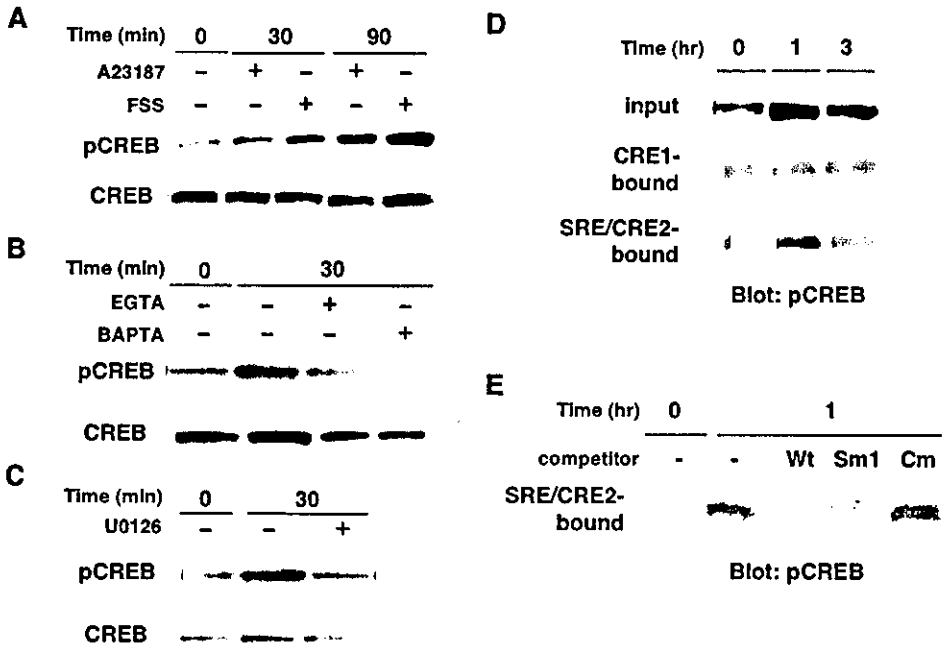

FIG. 7. **FSS causes phosphorylation of CREB, which binds to the CRE2 sequences, in a Ca^{2+}- and ERK-dependent manner.** Primary osteoblasts were subjected to FSS for the indicated times. Total cell lysates (*A–C*) or nuclear extracts (*D–E*) were prepared and analyzed by Western blot using antibodies against phosphorylated or total CREB (*A–C*) or analyzed for DNA binding by DNA precipitation followed by immunoblotting with phospho-CREB antibody. *A*, effect of FSS was compared with that of treatment with 100 nM A23187. *B*, FSS was applied in the presence of vehicle alone, 25 mM EGTA, or 50 μM BAPTA-AM. *C*, FSS was applied in the presence of vehicle alone or 10 μM U0126. *D*, nuclear extracts from cells subjected to FSS were analyzed for binding of phosphorylated CREB to CRE1 or SRE/CRE2 oligonucleotide probes by DNA precipitation assay. *E*, DNA precipitation assay for phospho-CREB binding to SRE/CRE2 were performed in the presence of free competitors including intact (*Wt*), SRE-mutated (*Sm1*), or CRE-mutated (*Cm*) SRE/CRE2 oligonucleotides.

to CRE1 was subloned into a reporter construct and tested for its transcriptional activity, neither the wild type nor a mutant construct showed a significant response to FSS (Fig. 6*A*). In contrast, SRE/CRE2 showed an ~4-fold induction by FSS, which was comparable with the induction observed with the longest 1.0-kb promoter (Fig. 6*B*). Mutational analysis indicated that none of three different mutations within the SRE sequences caused any major effects, whereas disrupting mutations in the CRE2 sequences caused an almost complete loss of response (Fig. 6*B*). These results indicate that the CRE2 sequences play a role in transcriptional induction of the *FosB/ΔFosB* gene by FSS.

Binding of Activated CREB to the CRE2 Element Is Critical to Transcriptional Induction of FosB/ΔFosB Gene by FSS—Our results have demonstrated that SRE/CRE2 sequences alone can confer an FSS response to a comparable extent to the full-length promoter and further suggest that the factor binding to the CRE2 site is critical to the transcriptional induction. We therefore examined whether CREB is activated and binds to this element in response to FSS. The results indicated that FSS, as well as a calcium ionophore, A23187, did induce CREB phosphorylation in osteoblasts (Fig. 7*A*), which occurred in a manner dependent on Ca^{2+} and ERK (Fig. 7, *B* and *C*). Moreover, DNA precipitation assays revealed that phosphorylated CREB induced by FSS did bind to the SRE/CRE2 sequences, but not to the CRE1 site (Fig. 7*D*). We also confirmed that binding of activated CREB to the SRE/CRE2 site occurred in a manner dependent on the CRE2 sequences by competition analysis (Fig. 7*E*). Taken together, these results suggest that FSS induces *FosB/ΔFosB* gene expression by activating CREB in a Ca^{2+}- and ERK-dependent manner, which then interacts with CRE2 to promote gene transcription.

Although our results demonstrate a role of CREB activation and subsequent binding to the CRE2 site, its relative importance in the context of full-length promoter remained obscure. Therefore, we applied an oligonucleotide decoy strategy to determine contribution of the SRE/CRE2 sequences to the transcriptional induction by FSS. We utilized circular dumbbell decoy oligonucleotides (CDODN) to inhibit binding of transcription factors to the SRE/CRE2 sequences. CDODN have been demonstrated to show efficient cellular uptake and increased stability (28, 29). We first confirmed by DNA precipitation assay that SRE/CRE2 CDODN actually bound activated CREB, whereas scrambled CDODN did not (Fig. 8*A*). Introduction of SRE/CRE2 CDODN into osteoblasts caused a dose-dependent inhibition of transcriptional induction by FSS. The maximal dose (10 μg/ml) caused nearly complete inhibition, indicating a major contribution of the transcription factors binding to the SRE/CRE2 site (Fig. 8*B*). Consistent with a critical role for CREB binding to the CRE2 site, we further demonstrated by mutant CDODN that the ability of SRE/CRE2 CDODN to inhibit FSS-induced *FosB/ΔFosB* gene transcription was dependent on the CRE2 sequences (Fig. 8*C*): an SRE-mutated SRE/CRE2 CDODN were still able to block the FSS response, whereas a CRE-mutated CDODN lost the ability to block *FosB* gene transcription. Moreover, we generated mutant promoter constructs in which either or both of the SRE and CRE2 sites were disrupted by site-directed mutagenesis and demonstrated that disruption of the CRE2 site in the context of the full-length promoter resulted in a significant reduction in the FSS response, whereas disruption of the SRE site showed a minimal effect (Fig. 8*D*). We therefore conclude that the CRE2 sequences at −407 in the upstream regulatory region of the *FosB/ΔFosB* gene make a major contribution to the transcriptional response to FSS in osteoblasts.

DISCUSSION

In the present study, we have demonstrated that FSS to osteoblasts induces *FosB/ΔFosB* gene expression via a Ca^{2+}/

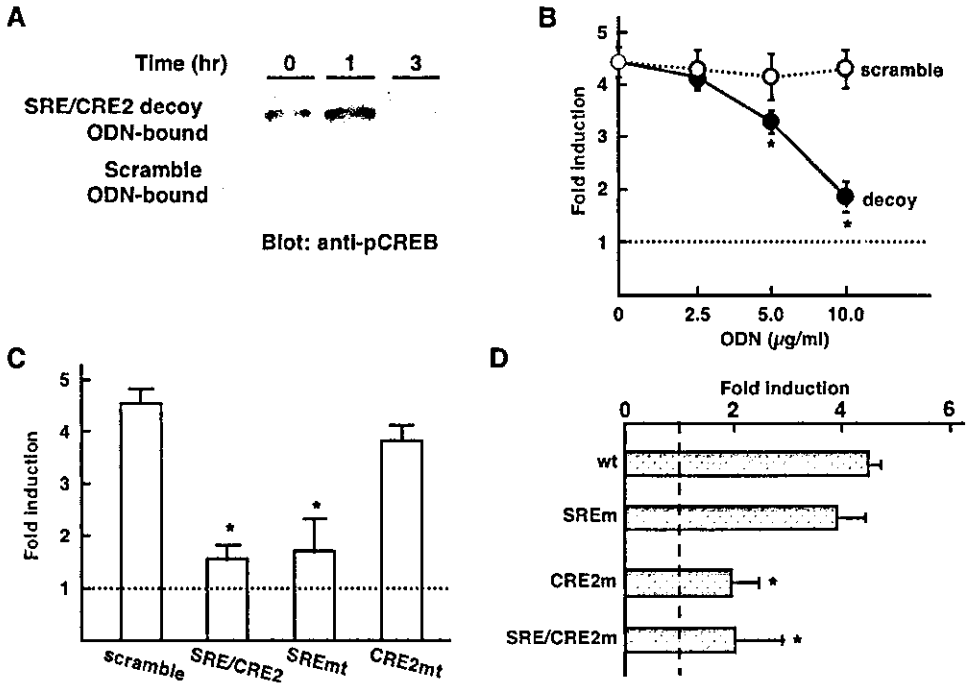

FIG. 8. **The CRE2 site plays a major role in FSS-induced transcription of *FosB/ΔFosB* gene.** *A*, primary osteoblasts were subjected to FSS for the indicated times. Nuclear lysates were prepared and analyzed for phospho-CREB binding to SRE/CRE2 or scrambled CDODN by DNA precipitation assay followed by Western blotting with anti-phospho-CREB antibody. *B*, primary osteoblasts were transfected with the luciferase reporter vector (*−1.0K*) together with various concentrations of SRE/CRE2 decoy or scramble CDODN, and induction of *FosB/ΔFosB* gene transcription by FSS was examined. Data were corrected for Renilla luciferase activity and expressed in -fold induction as a mean of results from four independent experiments with an error bar of S.D. *, significantly different ($p < 0.01$) from the value without decoy ODN. *C*, effect of 10 μg/ml scramble ODN, or intact, SRE-mutated or CRE2-mutated SRE/CRE2 CDODN was examined in the same way as *B*. *, significantly different ($p < 0.01$) from *scramble*. *D*, the wild-type 1.0-kb *FosB/ΔFosB* gene promoter construct (*wt*) and mutant plasmids with site-directed disrupting mutations at SRE (*SREm*), CRE2 (*CRE2m*), and both SRE and CRE2 (*SRE/CRE2m*) were transfected into primary osteoblasts, and analyzed for transcriptional response to FSS. Data were corrected for Renilla luciferase and expressed as -fold induction by FSS. *, significantly different ($p < 0.01$) from the wild type (*wt*) promoter.

ERK/CREB signaling pathway at the transcriptional level *in vitro*. FSS-activated CREB stimulated *FosB/ΔFosB* gene transcription through interaction with the CRE2 element, which appeared largely responsible for the FSS effect as demonstrated by DNA decoy experiments. Consistent with the direct transcriptional effect, induction of *FosB/ΔFosB* gene expression by mechanical forces was independent of prostaglandins known to induce c-Fos. We also confirmed that mechanical loading to bone caused accumulation of the ΔFosB protein *in vivo*. Because transgenic overexpression of ΔFosB has been shown to stimulate bone formation and thereby cause osteosclerosis in mice (18), increased expression of ΔFosB should contribute to mechanical stress-induced bone formation (Fig. 9).

ΔFosB is a C-terminal truncated *FosB* gene product generated by alternative splicing (15–17). Although physiological roles for ΔFosB are not fully understood, it has been proposed that ΔFosB is a molecular mediator of long-term neural and behavioral plasticity (35–37). In contrast to other Fos family members that are transiently induced in brain by various acute stimuli including electrical stimulation, stress, and psychotropic drugs, ΔFosB has been demonstrated to accumulate in specific regions of the brain after chronic administration of drugs of abuse and compulsive running (37). Moreover, *in vivo* overexpression of ΔFosB in brain resulted in augmented locomotor responses to cocaine administration and enhanced rewarding effects of cocaine and morphine, suggesting a role for ΔFosB in drug addiction (35). Directly relevant to our current study is the extremely stable nature of the ΔFosB protein (37). Based on the analogy of mechanical effect on bone to drug addiction in the sense that both are intermittent and repetitive in nature and are dependent on its magnitude and frequency (8), we propose that ΔFosB may also act as a molecular mediator of the mechanical loading effect on bone, which accumulates an intermittently loaded mechanical stress and further enhances mechanosensitivity. Validity of such a hypothesis is currently being tested in our laboratory.

A signaling pathway that involves Ca^{2+}, ERK, and CREB has already been described in other cell lineages (38–40). As a mechanism of ERK-dependent CREB activation, p90 ribosomal S6 protein kinase 1, a downstream effector of ERK, has been suggested to directly phosphorylate and activate CREB in human airway epithelial cells (41). And, although roles for CREB in bone formation remain to be established, a recent report has demonstrated that CREB is involved in transcriptional induction of cyclooxygenase-2 gene expression by FSS in a mouse osteoblastic cell line, acting in concert with C/EBP and AP-1 (30). Therefore, it is likely that the ERK/CREB pathway, which induces multiple transcriptional targets, constitutes a significant part of divergent intracellular signaling events induced by mechanical loading that leads to enhanced bone formation.

Initial characterization of the *FosB/ΔFosB* gene promoter (34) has revealed that the upstream regulatory region of the *FosB/ΔFosB* gene shares most critical transcription factor binding sites with that of *c-Fos* gene (11, 12): SRE and immediate downstream CRE/AP-1-like elements, which we designated CRE2 in the current paper, intervened by 6 nucleotides. Our results indicate that shear stress response elements in the *FosB/ΔFosB* promoter are present in a short region between −607 and −327 containing the above assumingly important sequences. This region considerably overlaps with recently reported mechanoresponsive regions in the *c-Fos* promoter (42). Because induction of FosB/*ΔFosB* gene transcription was de-

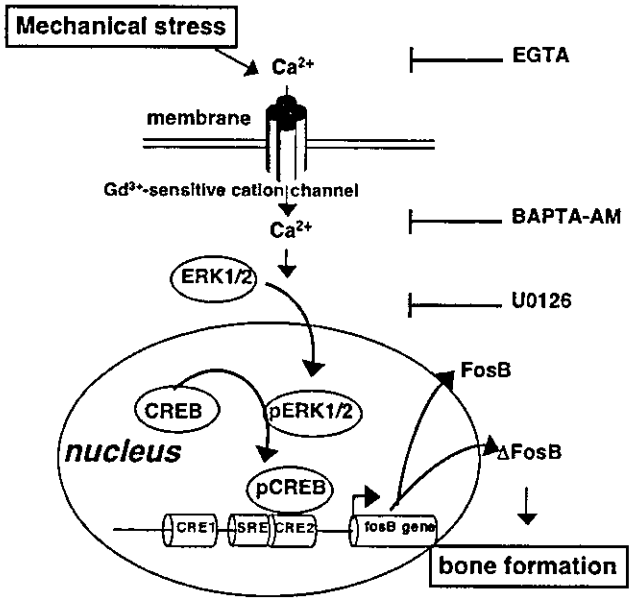

FIG. 9. **Transcriptional induction of *ΔFosB* expression as a mechanism of mechanical stress-induced bone formation.** Our results indicate that FSS induces *FosB*/*ΔFosB* gene transcription via a ERK/CREB pathway initiated by Ca^{2+} influx through Gd^{3+}-sensitive cation channel. The resultant increase in ΔFosB protein expression should lead to stimulation of bone formation and thereby increased bone mass as demonstrated by transgenic animal studies.

pendent on ERK, we initially reasoned that ERK activation of the TCF/SRF complex, which plays a major role in *c-Fos* gene regulation, would also be a critical determinant of *FosB*/*ΔFosB* responses to the mechanical stress. The role of SRF has already been suggested in stretch-induced *c-Fos* gene transcription in cardiomyocytes (43). And we found that FSS indeed activated transcription driven by the *c-Fos* gene-derived authentic SRE in our experimental system (data not shown). Consistently, SRE/CRE2, a stretch of sequences spanning both SRE and the immediate downstream CRE/AP-1 (CRE2) site, appeared effective and important in FSS responses of the *FosB*/*ΔFosB* gene promoter. In contrast to *c-Fos* SRE, however, disruption of SRE by substitutional mutation did not cause any appreciable effects on SRE/CRE2-driven transcription. These somewhat surprising results may be consistent with a previous report that *FosB* SRE is weaker than that of *c-Fos* (34). Our experiments with CDODN further demonstrated that a wild type and SRE-mutated SRE/CRE2 CDODN equally inhibited transcriptional activity of the long *FosB*/*ΔFosB* promoter. Therefore, *FosB*/*ΔFosB* gene seems to be subject to a distinct mode of transcriptional regulation compared with the *c-Fos* gene. Although the mechanisms by which ΔFosB stimulates bone formation remain to be elucidated, the unique mode of transcriptional regulation and the extraordinarily stable nature of ΔFosB will form a molecular basis to develop a new osteotropic drug that targets selective induction of ΔFosB in bone.

Acknowledgments—We thank Japan Tobacco Inc. for kindly providing the selective COX-2 inhibitor, JTE-522. We are also grateful to Drs. S. Tanaka and H. Katagiri (University of Tokyo) for adenoviral vectors.

REFERENCES

1. Morey, E. R., and Baylink, D. J. (1978) *Science* **201,** 1138–1141
2. Schneider, V., Oganov, V., LeBlanc, A., Rakmonov, A., Taggart, L., Bakulin, A., Huntoon, C., Grigoriev, A., and Varonin, L. (1995) *Acta Astronaut.* **36,** 463–466
3. Inoue, M., Tanaka, H., Moriwake, T., Oka, M., Sekiguchi, C., and Seino, Y. (2000) *Bone (N.Y.)* **26,** 281–286
4. Burr, D. B., Robling, A. G., and Turner, C. H. (2002) *Bone (N.Y.)* **30,** 781–786
5. Knothe Tate, M. L. (2003) *J. Biomech.* **36,** 1409–1424
6. Mikuni-Takagaki, Y. (1999) *J. Bone Miner. Metab.* **17,** 57–60
7. Nomura, S., and Takano-Yamamoto, T. (2000) *Matrix Biol.* **19,** 91–96
8. Ehrlich, P. J., and Lanyon, L. E. (2002) *Osteoporos. Int.* **13,** 688–700
9. Lean, J. M., Mackay, A. G., Chow, J. W., and Chambers, T. J. (1996) *Am. J. Physiol.* **270,** E937–E945
10. Karin, M., Liu, Z., and Zandi, E. (1997) *Curr. Opin. Cell Biol.* **9,** 240–246
11. Treisman, R. (1995) *EMBO J.* **14,** 4905–4913
12. Whitmarsh, A. J., and Davis, R. J. (1996) *J. Mol. Med.* **74,** 589–607
13. Li, C., and Xu, Q. (2000) *Cell. Signal.* **12,** 435–445
14. Grigoriadis, A. E., Schellander, K., Wang, Z. Q., and Wagner, E. F. (1993) *J. Cell Biol.* **122,** 685–701
15. Mumberg, D., Lucibello, F. C., Schuermann, M., and Muller, R. (1991) *Genes Dev.* **5,** 1212–1223
16. Yen, J., Wisdom, R. M., Tratner, I., and Verma, I. M. (1991) *Proc. Natl. Acad. Sci. U. S. A.* **88,** 5077–5081
17. Nakabeppu, Y., and Nathans, D. (1991) *Cell* **64,** 751–759
18. Sabatakos, G., Sims, N. A., Chen, J., Aoki, K., Kelz, M. B., Amling, M., Bouali, Y., Mukhopadhyay, K., Ford, K., Nestler, E. J., and Baron, R. (2000) *Nat. Med.* **6,** 985–990
19. Kveiborg, M., Chiusaroli, R., Sims, N. A., Wu, M., Sabatakos, G., Horne, W. C., and Baron, R. (2002) *Endocrinology* **143,** 4304–4309
20. Sims, N. A., Sabatakos, G., Chen, J. S., Kelz, M. B., Nestler, E. J., and Baron, R. (2002) *Bone (N.Y.)* **30,** 32–39
21. Matsushita, M., Masaki, M., Yagi, Y., Tanaka, T., and Wakitani, K. (1997) *Inflamm. Res.* **46,** 461–466
22. Ono, K., Akatsu, T., Murakami, T., Kitamura, R., Yamamoto, M., Shinomiya, N., Rokutanda, M., Sasaki, T., Amizuka, N., Ozawa, H., Nagata, N., and Kugai, N. (2002) *J. Bone Miner. Res.* **17,** 774–781
23. Sakata, T., Sakai, A., Tsurukami, H., Okimoto, N., Okazaki, Y., Ikeda, S., Norimura, T., and Nakamura, T. (1999) *J. Bone Miner. Res.* **14,** 1596–1604
24. Matsumoto, T., Nakayama, K., Kodama, Y., Fuse, H., Nakamura, T., and Fukumoto, S. (1998) *Bone (N.Y.)* **22,** 89S–93S
25. Inoue, D., Santiago, P., Horne, W. C., and Baron, R. (1997) *J. Biol. Chem.* **272,** 25386–25393
26. Sakai, K., Mohtai, M., Shida, J., Harimaya, K., Benvenuti, S., Brandi, M. L., Kukita, T., and Iwamoto, Y. (1999) *J. Bone Miner. Res.* **14,** 2089–2098
27. Inoue, D., Reid, M., Lum, L., Kratzschmar, J., Weskamp, G., Myung, Y. M., Baron, R., and Blobel, C. P. (1998) *J. Biol. Chem.* **273,** 4180–4187
28. Ahn, J. D., Kim, C. H., Magae, J., Kim, Y. H., Kim, H. J., Park, K. K., Hong, S., Park, K. G., Lee, I. K., and Chang, Y. C. (2003) *Biochem. Biophys. Res. Commun.* **310,** 1048–1053
29. Lee, I. K., Ahn, J. D., Kim, H. S., Park, J. Y., and Lee, K. U. (2003) *Curr. Drug Targets* **4,** 619–623
30. Ogasawara, A., Arakawa, T., Kaneda, T., Takuma, T., Sato, T., Kaneko, H., Kumegawa, M., and Hakeda, Y. (2001) *J. Biol. Chem.* **276,** 7048–7054
31. Weinreb, M., Rutledge, S. J., and Rodan, G. A. (1997) *Bone (N. Y.)* **20,** 347–353
32. Takahashi, M., Ishida, T., Traub, O., Corson, M. A., and Berk, B. C. (1997) *J. Vasc. Res.* **34,** 212–219
33. You, J., Reilly, G. C., Zhen, X., Yellowley, C. E., Chen, Q., Donahue, H. J., and Jacobs, C. R. (2001) *J. Biol. Chem.* **276,** 13365–13371
34. Lazo, P. S., Dorfman, K., Noguchi, T., Mattei, M. G., and Bravo, R. (1992) *Nucleic Acids Res.* **20,** 343–350
35. Kelz, M. B., Chen, J., Carlezon, W. A., Jr., Whisler, K., Gilden, L., Beckmann, A. M., Steffen, C., Zhang, Y. J., Marotti, L., Self, D. W., Tkatch, T., Baranauskas, G., Surmeier, D. J., Neve, R. L., Duman, R. S., Picciotto, M. R., and Nestler, E. J. (1999) *Nature* **401,** 272–276
36. Nestler, E. J., Kelz, M. B., and Chen, J. (1999) *Brain Res.* **835,** 10–17
37. Nestler, E. J., Barrot, M., and Self, D. W. (2001) *Proc. Natl. Acad. Sci. U. S. A.* **98,** 11042–11046
38. Ohkubo, N., Mitsuda, N., Tamatani, M., Yamaguchi, A., Lee, Y. D., Ogihara, T., Vitek, M. P., and Tohyama, M. (2001) *J. Biol. Chem.* **276,** 3046–3053
39. Zanassi, P., Paolillo, M., Feliciello, A., Avvedimento, E. V., Gallo, V., and Schinelli, S. (2001) *J. Biol. Chem.* **276,** 11487–11495
40. Nashat, A. H., and Langer, R. (2003) *Mol. Cell. Biol.* **23,** 4788–4795
41. Song, K. S., Seong, J. K., Chung, K. C., Lee, W. J., Kim, C. H., Cho, K. N., Kang, C. D., Koo, J. S., and Yoon, J. H. (2003) *J. Biol. Chem.* **278,** 34890–34896
42. Peake, M. A., and El Haj, A. J. (2003) *FEBS Lett.* **537,** 117–120
43. Sadoshima, J., and Izumo, S. (1993) *Circ. Res.* **73,** 424–438
44. Miyazaki, T., Katagiri, H., Kanegae, Y., Takayanagi, H., Sawada, Y., Yamamoto, A., Pando, M. P., Asano, T., Verma, I. M., Oda, H., Nakamura, K., and Tanaka, S. (2000) *J. Cell Biol.* **148,** 333–342

0013-7227/03/$15.00/0
Printed in U.S.A.

Endocrinology 144(12):5138–5144

doi: 10.1210/en.2003-0502

Deletion of Vitamin D Receptor Gene in Mice Results in Abnormal Skeletal Muscle Development with Deregulated Expression of Myoregulatory Transcription Factors

ITSURO ENDO, DAISUKE INOUE, TAKAO MITSUI, YOSHIFUMI UMAKI, MASASHI AKAIKE, TATSUYA YOSHIZAWA, SHIGEAKI KATO, AND TOSHIO MATSUMOTO

Department of Medicine and Bioregulatory Sciences (I.E., D.I., T.Mi., Y.U., M.A., T.Ma.), University of Tokushima Graduate School of Medicine, Tokushima 770-8503, Japan; and Institute of Molecular and Cellular Biosciences (T.Y., S.K.), University of Tokyo, Tokyo 113-0032, Japan

Although rachitic/osteomalacic myopathy caused by impaired vitamin D actions has long been described, the molecular pathogenesis remains elusive. To determine physiological roles of vitamin D actions through vitamin D receptor (VDR) in skeletal muscle development, we examined skeletal muscle in VDR gene deleted (VDR −/−) mice, an animal model of vitamin D-dependent rickets type II, for morphological changes and expression of myoregulatory transcription factors and myosin heavy chain isoforms. We found that each muscle fiber was small and variable in size in hindlimb skeletal muscle from VDR −/− mice, although overall myocyte differentiation occurred normally. These abnormalities were independent of secondary metabolic changes such as hypocalcemia and hypophosphatemia, and were accompanied by aberrantly high and persistent expression of myf5, myogenin, E2A, and early myosin heavy chain isoforms, which are normally down-regulated at earlier stages. Moreover, treatment of VDR-positive myoblastic cells with $1,25(OH)_2D_3$ *in vitro* caused down-regulation of these factors. These results suggest that VDR plays a physiological role in skeletal muscle development, participating in temporally strict down-regulation of myoregulatory transcription factors. The present study can form a molecular basis of VDR actions on muscle and should help further establish the physiological roles of VDR in muscle development as well as pharmacological effects of vitamin D on muscle functions. (*Endocrinology* 144: 5138–5144, 2003)

THE ACTIVE FORM of vitamin D, 1α,25-dihydroxyvitamin D [$1,25(OH)_2D$], is a major calcium-regulating hormone that is indispensable for maintenance of calcium and bone homeostasis and acts through binding to the vitamin D receptor (VDR) that belongs to the nuclear receptor superfamily. Various disorders with impaired vitamin D actions, including vitamin D deficiency, genetic defects in the vitamin D-activating enzyme, 25-hydroxyvitamin D 1α-hydroxylase, or in the vitamin D receptor (VDR) lead to rickets or osteomalacia characterized by hypocalcemia, hypophosphatemia, secondary hyperparathyroidism, and bone abnormalities due to mineralizing defects (1–3). Moreover, VDR is known to be expressed in a wide spectrum of tissues unrelated to calcium and bone metabolism, and accordingly, vitamin D has been shown to modulate fundamental cellular processes such as proliferation, differentiation, and survival of various cell lineages *in vitro* (4, 5). However, physiological relevance of such vitamin D effects *in vivo* has not yet been established, nor has the role of VDR.

Clinical evidence suggests that vitamin D may play a role in muscle metabolism and function. Progressive weakness and wasting of skeletal muscle have been demonstrated in patients with rickets or osteomalacia (6, 7). In addition, it has been shown that VDR is expressed at particular stages of differentiation from myoblasts to myotubes (8–10), implying that skeletal muscle may potentially be a physiological target of $1,25(OH)_2D$. However, the mechanism of rachitic/osteomalacic myopathy is not fully understood, and it is currently unclear whether muscle abnormalities in those patients are a direct consequence of impaired vitamin D actions in muscle or a result of secondary systemic changes such as hypocalcemia, hypophosphatemia, and elevated PTH levels in the circulation.

To address these issues *in vivo*, we examined morphological abnormalities of skeletal muscle in VDR gene-null mutant (VDR −/−) mice that recapitulated a human disease of vitamin D resistance, vitamin D-dependent rickets type II (11). At the same time, we investigated expression of myogenic regulatory factors such as Myf5, myogenin, MyoD, MRF4, and E2A (12, 13) that play critical roles in myoblast differentiation and skeletal muscle development. We also examined myosin heavy chain (MHC) isoforms including embryonic, neonatal, and adult fast types (14) as differentiation markers that are expressed in a stage-specific manner during muscle development. In addition, we examined $1,25(OH)_2D$ effects on expression of these genes by a mouse myoblast cell line, C2C12, to analyze direct vitamin D actions on muscle cells *in vitro*. We hereby present evidence that VDR plays a pivotal role in the maintenance of homeostasis in fully differentiated skeletal muscle cells, supporting our hypothesis that muscle is a direct physiological target of VDR-dependent vitamin D actions.

Abbreviations: $1,25(OH)_2D$, 1α,25-Dihydroxyvitamin D; MHC, myosin heavy chain; SSC, sodium chloride-sodium citrate; VDR, vitamin D receptor.

Materials and Methods

Animals and cell cultures

Generation of VDR gene deleted mice has been described (11). C2C12, a mouse myoblast cell line, was purchased from Riken cell bank (Tsukuba, Japan) and maintained in DMEM supplemented with 10% fetal bovine serum and penicillin/streptomycin (Life Technologies, Rockville, MD). For experiments, 80% confluent C2C12 cells were treated with vehicles alone or 10 nM $1,25(OH)_2D_3$ for 48–96 h and harvested for further analysis.

Chemicals and antibodies

All the reagents were obtained from Sigma (St. Louis, MO) unless otherwise indicated. Antibodies against Myf5, MyoD, MRF4, E2A, Id1, and Id2 were purchased from Santa Cruz Biotechnology (Santa Cruz, CA), those against myogenin and MHC of embryonic type from American Research Products, Inc. (Belmont, MA), and those against MHC of neonatal and adult fast type from Medac Diagnostika (Hamburg, Germany).

Histological analysis

Samples were isolated from hindlimb skeletal muscle of 3- and 8-wk-old VDR knockout (−/−) mice and wild-type control littermates, rapidly frozen in liquid nitrogen-cooled isopentane (2-methylbutane), sectioned, and stored in liquid nitrogen. Muscle tissue sections were subjected to hematoxylin/eosin staining as follows. Serial sections of frozen muscle with 6-μm thickness were first incubated with Mayer's hematoxylin solution for 5 min, washed in distilled deionized water, and then incubated with 0.5% eosin solution for 3 min. Sections were washed three times in distilled deionized water and once in ethanol, dehydrated, and mounted. Diameters of muscle fibers were measured in photomicrographs of hematoxylin/eosin-stained muscle tissue sections.

Immunostaining

Serial sections of frozen muscle with 6-μm thickness were fixed for 20 min with PBS containing 4% paraformaldehyde and first incubated with a primary antibody at room temperature for 1 h. Sections were washed three times in PBS, incubated with biotin-conjugated secondary antibodies for 1 h, and then with ABC solution (Vector Laboratories, Burlingame, CA) diluted 100-fold in PBS. For detection, the samples were incubated for 5–20 min with 0.5 mg/ml diaminobenzidine solution or p-nitro blue tetrazolium/5-bromo-4-chloro-3-indolyl phosphate solution (Life Technologies, Rockville, MD), washed twice in distilled deionized water, mounted, and observed under a microscope.

RT-PCR analysis

Total RNA from skeletal muscle tissues and C2C12 cells were isolated by using RNeasy Mini Kit (QIAGEN GmbH, Hilden, Germany) or TRIzol reagent (Invitrogen, Carlsbad, CA). One microgram total RNA was reverse-transcribed by incubating in a 20-μl reaction containing random primers (Promega; 0.5 mg/ml, 2 μl), reverse transcriptase buffer (Promega; 2 μl), deoxynucleoside triphosphates (2.5 mM each), 20 U RNase inhibitor (Promega), and 20 U reverse transcriptase (Promega) for 10 min at room temperature, 60 min at 42 C, and 5 min at 95 C. PCR was performed using various sets of primers shown in Table 1. One microliter of 20 μl reverse transcription reactions was denatured for 2 min at 95 C, followed by 28–35 cycles (except for 23 cycles with glyceraldehyde-3-phosphate dehydrogenase) of amplification: 2 min at 95 C, 30 sec at 57–61 C, and 30 sec at 72 C. PCR products were electrophoretically separated on 2% agarose gels and visualized with ethidium bromide staining.

Northern blot analysis

Total RNA (20 μg) was separated on a 1% agarose gel containing 6% formaldehyde and transferred to HYBOND+ nylon membrane (Amersham, Little Chalfont, Buckinghamshire, UK) by capillary action in 20× sodium chloride-sodium citrate (SSC) buffer (3 M NaCl, 0.3 M sodium citrate, pH 7.0). RNA was cross-linked to the membrane using the UV Cross-Linker (model CX-2000, UVP, Upland, CA). An equal amount of RNA loading and transfer was confirmed by ethidium bromide staining and UV visualization of ribosomal RNAs (data not shown). Hybridization was performed with a nonisotopic digoxigenin labeling system using DIG PCR Probe Synthesis Kit and DIG Easy Hyb (Roche Diagnostics, Indianapolis, IN). Briefly, the membranes were first prehybridized in the DIG Easy Hyb buffer for 30 min at 42 C, then hybridized in DIG Easy Hyb buffer with an appropriate probe generated by DIG PCR Probe Synthesis Kit for 16 h at 42 C, washed twice in 2× SSC/0.1% sodium dodecyl sulfate at room temperature for 5 min and twice in 0.2% SSC/0.1% sodium dodecyl sulfate at 50 C for 15 min, and exposed to films. PCR primers used to generate cDNA probes for Northern blot analysis were as follows: 5′-gcatgcaaggtgtgtaagaggaag-3′ and 5′-ggctgttttctggacatcaggaca-3′ for myogenin (593 base); 5′-aagagaggtatcctgaccctgaag-3′ and 5′-cttgatcttcatggtgctaggagc-3′ for β-actin (801 base); and 5′-aaccaagctttcgagacgctcaag-3′ and 5′-aaaagaacaggcagaggagaaccc-3′ for Myf5 (664 base). The expected size of the obtained cDNA probes is shown in *parentheses*. In some experiments, poly A^+ RNA was obtained with PolyATract mRNA Isolation systems (Promega) following the manufacturer's instruction and analyzed by Northern blot analysis.

TABLE 1. List of PCR primers used in this study

Gene	Primer	Accession no.
Myf5	F: 5′-tgtatcccctcaccagaggat-3′	58-78; XM192677
	R: 5′-ggctgtaatagttctccacctgtt-3′	442-419; XM192677
Myogenin	F: 5′-gagcgcgatctccgctacagagg-3′	470-492; NM031189
	R: 5′-ctggcttgtggcagcccagg-3′	849-830; NM031189
E2A (E12)	F: 5′-agacgaggacgaggacgaccttc-3′	130-152; D29919
E2A (E47)	F: 5′-ccagcagtacagatgaggtgctg-3′	1660-1682; AF352579
E2A (common)	R: 5′-acgccagacaccttctcctcctc-3′	426-404; D29919/ 1954-1932; AF352579
Id	F: 5′-gcctgttctcaggatcatgaaggt-3′	71-94; XM203819
	R: 5′-tgcaggtccctgatgtagtcgatt-3′	382-359; XM203819
MyoD	F: 5′-ctcctttgagacagcagacgactt-3′	254-277; M84918
	R: 5′-aaatcgcattggggtttgagcctg-3′	1134-1111; M84918
MRF4	F: 5′-gagggtgcggatttcctgcgcacc-3′	571-548; NM008657
	R: 5′-aagggctgaggcatccacgtttgc-3′	664-641; NM008657
MHCneonatal	F: 5′-acgcaatgctgaggctgttaaagg-3′	5729-5753; XM204651
	R: 5′-agtaaacccagagaggcaagtgac-3′	370-346; M12289
VDR	F: 5′-cctcactggacatgatggaaccg-3′	668-690; NM009504
	R: 5′-gatgtaggtctgcagcgtgttgg-3′	1194-1172; NM009504
G3PDH	F: 5′-tgaaggtcggtgtgaacggatttggc-3′	51-76; NM008084
	R: 5′-catgtaggccatgaggtccaccac-3′	1033-1010; NM008084

F, Forward; R, reverse.

Results

Abnormal skeletal muscle development in VDR −/− mice

To test a hypothesis that VDR has a physiological role in skeletal muscle development, we first examined skeletal muscle tissues from VDR −/− mice for morphological abnormalities. As previously described (11), the VDR −/− mice grow normally until weaning and thereafter develop various metabolic abnormalities including hypocalcemia, hypophosphatemia, secondary hyperparathyroidism, and bone deformity as typical features of rickets. At the age of 3 wk, there were no significant differences between VDR−/− and VDR+/+ mice in body weight or serum concentrations of calcium, phosphate, alkaline phosphatase, 25(OH)D, 24,25(OH)D or $1,25(OH)_2D$. To exclude any deleterious effects of such secondary systemic metabolic changes on muscle, we analyzed 3-wk-old mice just before weaning that showed no apparent biochemical or morphological abnormalities. As shown in Fig. 1, each muscle fiber obtained from quadriceps femoris muscle of VDR −/− mice (Fig. 1A) appeared smaller than that of wild-type (VDR+/+) mice (Fig. 1B) at 3 wk. Quantitative analysis showed that skeletal muscle cell diameters in VDR −/− mice at 3 wk were significantly decreased by approximately 20% on the average and appeared to be more widely distributed compared with those in wild-type mice (Fig. 2). The morphological changes were more prominent in 8-wk-old VDR −/− mice (Fig. 1C) compared with VDR+/+ controls of the same age (Fig. 1D), suggesting either a progressive nature of the abnormalities caused by the absence of VDR or additive effects of systemic metabolic changes already present at this age. Neither degenerative nor necrotic changes were observed in VDR −/− skeletal muscle. Similar results were obtained with biceps femoris, medial gastrocnemius, anterior tibial, and soleus muscles, indicating that the muscle abnormalities in VDR −/− mice occurred diffusely without any preference to type I or type II fibers. These results demonstrate that VDR is involved in physiological regulation of skeletal muscle development. Our observations further suggested that although overall differentiation steps into myocytes occurred normally, the absence of VDR caused abnormalities probably in late stages of myocyte maturation and/or in metabolism of mature myocytes.

Deregulated expression of myogenic regulatory factors in VDR −/− mice

To obtain insight into the mechanism of muscle abnormalities observed in VDR −/− mice, we examined expression of myogenic differentiation factors including MyoD family of transcription factors with muscle contractile proteins, *i.e.* embryonic, neonatal, and adult fast (type II) isoforms of MHC. Immunohistochemical analysis of quadriceps femoris muscle from 3-wk-old mice revealed persistently increased expression of myf5 (Fig. 3A), E2A (Fig. 3B), and myogenin (Fig. 3C), all of which were minimally expressed in muscle from VDR +/+ mice at this age (Fig. 3, F–H). No apparent differences were observed in expression of MyoD (Fig. 3, D and I) and MRF4 (Fig. 3, E and J). Consistent with the deregulated expression of myogenic transcription factors that control muscle phenotype, we also observed aberrantly increased expression of embryonic (Fig. 4A) and neonatal type MHC (Fig. 4B) in the cytoplasm of small muscle fibers of quadriceps femoris muscle from 3-wk-old VDR −/− mice, whereas type II (adult fast) MHC expression in VDR −/− muscle was the same as VDR +/+ controls (Fig. 4, C and F). At the age of 8 wk, although the embryonic MHC had disappeared, persistent expression of neonatal MHC was still detectable in VDR −/− mice (data not shown). There were no differences in expression levels of Id1 and Id2, known targets of vitamin D (15) in either 3- or 8-wk-old mice (data not shown). All the above findings were confirmed at the mRNA level as shown in Fig. 5: expression of myf5, myogenin, E12 and E47, both of which are produced from the same E2A gene, and neonatal MHC mRNA was higher in VDR −/− mice than that of VDR +/+ mice at 3 and 8 wk. VDR mRNA was only detectable in 3-wk-old wild-type muscle under our experimental conditions. These results are consistent with the notion that the absence of VDR disturbs the coordinate pattern of expression of myogenic transcription factors during myocyte development, causing altered levels of differentiation-associated, lineage-specific gene expression and thereby morphological abnormalities. The possibility that these alterations were secondary effects of systemic changes appeared unlikely, because abnormalities in both morphology and MyoD family expression were observed already in 3-wk-old VDR −/− mice and also in mice

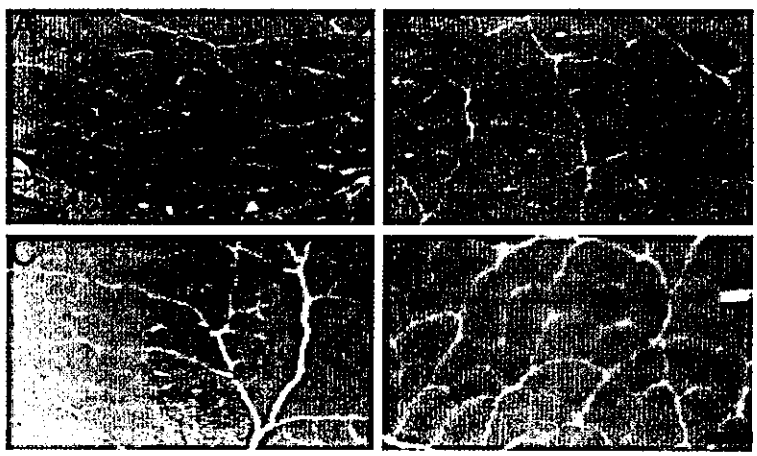

FIG. 1. Morphological abnormalities of skeletal muscle tissue from VDR −/− mice. Three- or 8-wk-old VDR −/− and +/+ (wild-type littermate) mice were euthanized, and quadriceps femoris muscle tissues were obtained. Fresh-frozen sections were stained with hematoxylin/eosin as described in *Materials and Methods* and observed under microscope. *Scale bar*, 20 μm. A, Three-week-old VDR −/− mice; B, 3-wk-old VDR +/+ mice; C, 8-wk-old VDR −/− mice; D, 8-wk-old VDR +/+ mice. Similar changes in muscle fiber size were also observed in biceps femoris, medial gastrocnemius, anterior tibial, and soleus muscles (data not shown).

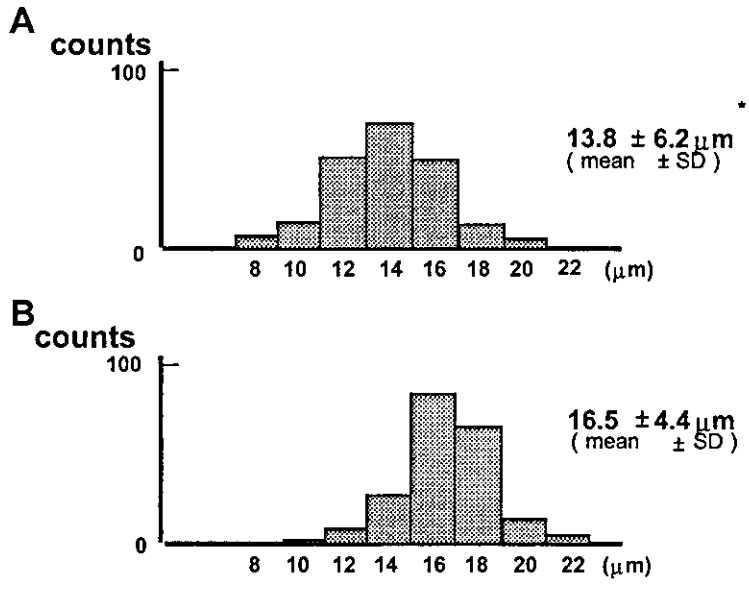

FIG. 2. VDR −/− muscle fibers are small and variable in size. Diameter of muscle fibers in 3-wk-old VDR −/− (A) and VDR +/+ (B) mice was measured in microphotograph of the hematoxylin/eosin-stained tissue sections. Two hundred cells were randomly counted, and data were expressed in histogram and as mean size ± SD. *, Significantly different from VDR +/+ wild-type littermates.

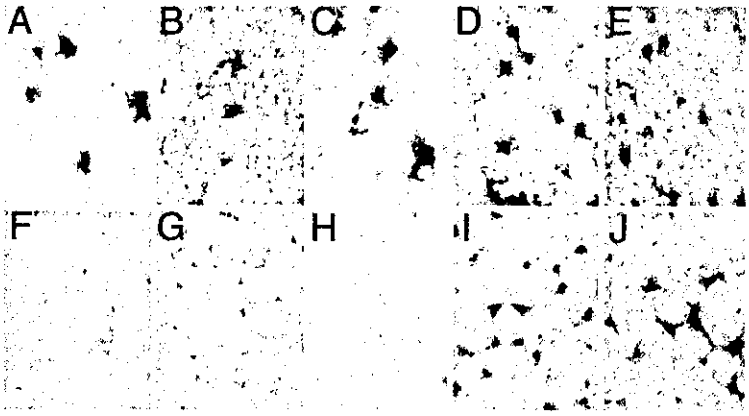

FIG. 3. Immunohistochemical analysis of MyoD family transcription factors in skeletal muscle tissues of 3-wk-old mice. Quadriceps femoris muscle tissue sections of 3-wk-old VDR −/− (A–E) and VDR +/+ (F–J) mice were analyzed by immunohistochemistry for expression of Myf5 (A and F), E2A (B and G), myogenin (C and H), MyoD (D and I), and MRF4 (E and J) as described in *Materials and Methods*. Expression of myf5, E2A, and myogenin was only detectable in VDR −/− muscles, which was mostly localized in nuclear and perinuclear regions. Virtually the same results were obtained in biceps femoris, medial gastrocnemius, anterior tibial, and soleus muscles (data not shown).

fed with high-calcium diet to rescue the phenotype of rickets that showed normal circulating levels of calcium, phosphate, and PTH (Ref. 11 and data not shown).

1,25(OH)$_2$D$_3$ down-regulates myf5 and myogenin expression by myoblasts in vitro

Our results suggest that temporally strict down-regulation of myogenic differentiation factors requires the presence of VDR. Therefore, we finally examined whether or not 1,25(OH)$_2$D$_3$ was able to directly down-regulate MyoD family gene expression in myocyte-lineage cells *in vitro*. C2C12 myoblasts were grown to 80% confluence and then treated with 10 nM 1,25(OH)$_2$D$_3$ or a vehicle alone in the presence of 10% charcoal-treated fetal bovine serum for 48–96 h. During this phase of initial differentiation, less than 5% of myotubes appeared (data not shown). There were no apparent differences in the overall differentiational process between vehicle-treated and 1,25(OH)$_2$D$_3$-treated cells. As shown in Fig. 6A, VDR mRNA was found to be expressed at constant levels throughout the experimental period. In control cells, myf5 was already expressed in growing cells, and the level of expression stayed the same. In contrast, expression of myogenin and neonatal type MHC showed a gradual increase in a time-dependent manner. Treatment with 10 nM 1,25(OH)$_2$D$_3$ for 48 h caused a decrease in the steady-state levels of myf5, myogenin, and neonatal MHC, and the 1,25(OH)$_2$D$_3$ effects lasted up to 96 h (Fig. 6A). The effects on myogenin and myf5 expression were also confirmed quantitatively by Northern blot analysis (Fig. 6, B and C). Thus, these *in vitro* results using myoblast cultures have in large part recapitulated our *in vivo* findings and are in agreement with our hypothesis that 1,25(OH)$_2$D participates in physiological regulation of muscle development, particularly playing a role in temporally strict down-regulation of some myogenic differentiation factors through VDR.

Discussion

Defects in VDR-dependent vitamin D actions cause rickets or osteomalacia. Although rachitic or osteomalacic myopathy has long been described, the molecular pathogenesis remains elusive. One of the central questions to be answered is whether the myopathy is caused by impairment of direct VDR-dependent actions of active vitamin D on muscle or by secondary metabolic changes including hypocalcemia, hy-

FIG. 4. Immunohistochemical analysis of MHC isoforms in skeletal muscle tissues of 3-wk-old mice. Quadriceps femoris muscle tissue sections of 3-wk-old VDR −/− (A–C) and VDR +/+ (D–F) mice were analyzed by immunohistochemistry for expression of MHC of embryonic type (A and D), neonatal type (B and E), and adult fast type (type II) (C and F), as described in *Materials and Methods*. In the lower half of panels A and D, nonspecific staining of the intercellular space without specific primary antibodies (2° only) is shown. Also note that in panels C and F, some type I fibers scattered in the field are devoid of staining in contrast to the diffuse cytoplasmic staining of surrounding type II fibers. *Scale bar*, 40 μm.

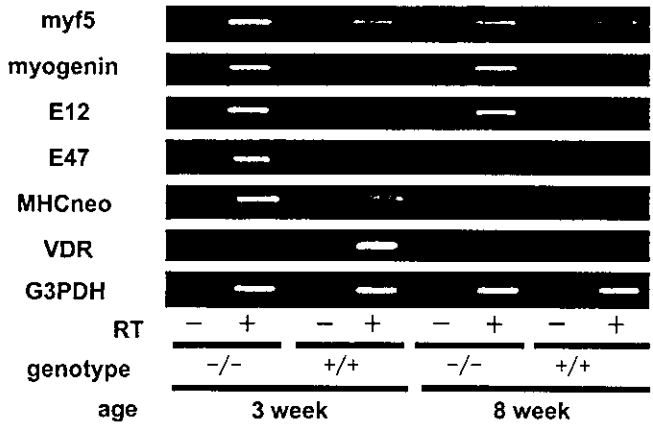

FIG. 5. Expression of MyoD family and MHC mRNA in skeletal muscle from VDR −/− and +/+ mice. Expression of myf5, myogenin, E2A, neonatal type MHC, and VDR mRNA in hindlimb skeletal muscle was analyzed by RT-PCR in 3- and 8-wk-old VDR −/− and +/+ mice as described in *Materials and Methods*. For each PCR, a negative control without reverse transcriptase is also shown.

pophosphatemia, and hyperparathyroidism. Some clinical studies have indicated that the extent of hypocalcemia and/or hypophosphatemia does not correlate well with the severity of myopathy and that correction of hypocalcemia does not lead to a cure of the muscle symptoms (16), which supports an involvement of direct VDR actions. However, others have demonstrated that PTH excess leads to similar muscle atrophy and weakness causing increased intracellular calcium (17) and impaired production of contractile proteins (18). Efforts to obtain conclusive results have been hampered by an inability to test direct effects of VDR in human muscles and absence of appropriate animal models of rickets for this purpose.

We have recently generated VDR gene deleted mice as an animal model of type II vitamin D-dependent rickets. VDR −/− mice almost completely recapitulated the human disease and showed most of the characteristic abnormalities including hypocalcemia, hypophosphatemia, secondary hyperparathyroidism, increased serum levels of 1,25D and alkaline phosphatase, decreased 24,25-dihydroxyvitamin D, and osteopathy (11). A unique feature in these model mice is that they grow normally and show no bone or metabolic abnormalities until they are weaned, presumably due to high calcium content or other critical nutrients in the breast milk. In the present study, we took advantage of this feature and were able to demonstrate that the absence of VDR causes muscle abnormality independently of secondary effects of systemic metabolic changes. Three lines of evidence from the present study support physiological roles of direct VDR actions on skeletal muscle: firstly, VDR −/− mice developed apparent morphological abnormalities in skeletal muscle and a deregulated pattern of muscle gene expression before weaning; secondly, the same changes were still observed in older rescued VDR −/− mice fed with high calcium diet; and thirdly, direct negative regulatory effects of $1,25(OH)_2D$ on muscle gene expression were at least in part reproduced in cultured myoblasts *in vitro*. Thus, our results suggest that the skeletal muscle is a direct physiological target of VDR actions and that the absence of VDR *in situ* caused muscle abnormalities in VDR −/− mice, although secondary changes such as hypocalcemia, hypophosphatemia, and hyperparathyroidism may contribute in an additive and/or modulatory manner.

As a clue to the mechanism whereby the absence of VDR caused skeletal muscle abnormalities, we found prolonged up-regulation of a certain subset of myogenic regulatory factors: myf5, myogenin, and E2A. The transcription factors of the MyoD family play pivotal roles in muscle cell differentiation. During muscle differentiation, the four members of the family thus far identified, myf5, MyoD, myogenin, and MRF4, show a temporal and sequential pattern of expression that is subject to complex mutual regulation and exhibit distinct but overlapping functions that are not yet completely understood (12, 19). Expression of muscle-specific genes including MHC subtypes is under the control of the MyoD family members (20–23). Although we currently have no evidence for a direct link between deregulated expression of myogenic transcription factors and the muscle phenotype observed in VDR −/− mice, it is plausible to assume that aberrant up-regulation of myf5, myogenin, and E2A leads to abnormal expression of MHC and muscle atrophy, because it appears that a strictly regulated, coordinate pattern of expression of the MyoD family defines the program of myocyte differentiation and maturation. Such an assumption is further supported by a previous report that transgenic myogenin overexpression in differentiated postmitotic muscle fibers in mice resulted in grossly normal muscle development but higher rates of neonatal mortality, probably due to mildly impaired muscle function (24).

The molecular mechanism by which myogenic transcription factors including myf5, myogenin, and E2A are aberrantly and persistently up-regulated is currently unknown. However, it is of note that, in the course of muscle differentiation, these genes are normally down-regulated during the stages in which VDR is expressed (25). We therefore assume that VDR is involved in transcriptional down-regulation of these genes during the process of physiological muscle differentiation. Our *in vitro* observations that

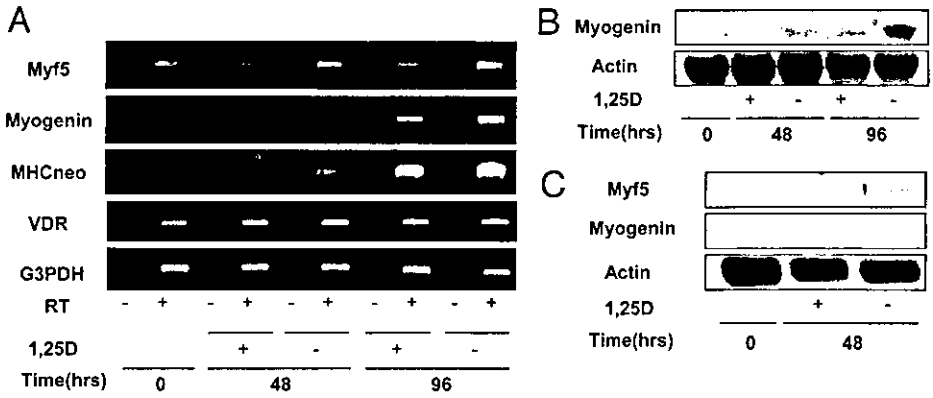

FIG. 6. Down-regulation of myf5, myogenin, and MHC neonatal type mRNA by 1,25D3 in C2C12 myoblastic cell line. A, 80% confluent C2C12 cells were treated with a vehicle alone or 10 nM 1,25D3 for indicated times and analyzed for mRNA expression of myf5, myogenin, MHC neonatal type, VDR and glyceraldehyde-3-phosphate dehydrogenase by RT-PCR as described in *Materials and Methods*. For each PCR, a negative control without reverse transcriptase is also shown. B, The same RNA samples as panel A were analyzed for myogenin and actin mRNA expression by Northern blot analysis as described under *Materials and Methods* to show quantitative difference. C, Poly A^+ RNA was purified as described under *Materials and Methods* and analyzed for expression of myf5, myogenin, and actin mRNA by Northern blot analysis.

$1,25(OH)_2D$ was able to down-regulate myf5, myogenin, and neonatal MHC mRNA expression in C2C12 myoblasts further support this idea. However, we have not been able to identify known negative vitamin D response elements (26–28) in the promoter region of myf5 and myogenin genes. Further functional analysis of the promoters of MyoD family members may elucidate the down-regulatory mechanism of these genes through VDR.

Our findings may be clinically relevant to the musculoskeletal health in the aged, because vitamin D insufficiency has been shown to be associated with lower muscle strength and increased falling tendency in adults. Conversely, supplement of native vitamin D or treatment with active vitamin D has been reported to improve muscle functions and protect from falling events and falling-associated fractures (29–33). Whether the beneficial effects of vitamin D treatment occur via direct VDR actions on skeletal muscle cells or indirect mechanisms remains unclear. Interestingly, however, abnormal expression of MyoD family members and MHC isoforms has been reported in various models of immobilization and denervation (34–38). Considering the plasticity and highly adaptive nature of muscle fibers, it is conceivable that reprogramming and adaptations of muscle fibers may occur under various pathological conditions, particularly in elderly patients, and that these processes may be modulated by VDR-dependent vitamin D actions.

In summary, we have shown that VDR gene deleted mice exhibit abnormal skeletal muscle development. These abnormalities occur independently of secondary metabolic changes such as hypocalcemia and hypophosphatemia and are accompanied by deregulated expression of myogenic transcription factors and MHC isoforms. These effects appear to involve direct vitamin D actions on muscle through VDR, because similar effects were reproduced by treatment of VDR-positive myoblastic cells with $1,25(OH)_2D$ *in vitro*. The present study can form a molecular basis of VDR actions on muscle and should help further establish the physiological roles of VDR in muscle development as well as pharmacological effects of vitamin D on muscle functions.

Acknowledgments

We thank Kiyomi Yoshida for her helpful assistance in preparation of the manuscript.

Received April 21, 2003. Accepted August 7, 2003.

Address all correspondence and requests for reprints to: Daisuke Inoue, M.D., Department of Medicine and Bioregulatory Sciences, University of Tokushima Graduate School of Medicine, 3-18-15 Kuramoto-Cho, Tokushima 770-8503, Japan. E-mail: inoued@clin.med.tokushima-u.ac.jp.

This work was supported in part by Grants-in-Aid for Scientific Research on Priority Areas 12137207 (to T.Ma.) and Grants-in-Aid for Scientific Research (B) (to T.Ma.) from the Ministry of Education, Science, Sports and Culture of Japan; and Fellowships from Japan Intractable Diseases Research Foundation (to D.I.).

References

1. **Kato S, Yoshizazawa T, Kitanaka S, Murayama A, Takeyama K** 2002 Molecular genetics of vitamin D-dependent hereditary rickets. Horm Res 57: 73–78
2. **Pettifor JM** 2002 Rickets. Calcif Tissue Int 70:398–399
3. **Hutchison FN, Bell NH** 1992 Osteomalacia and rickets. Semin Nephrol 12: 127–145
4. **Walters MR** 1992 Newly identified actions of the vitamin D endocrine system. Endocr Rev 13:719–764
5. **Stumpf WE** 1995 Vitamin D sites and mechanisms of action: a histochemical perspective. Reflections on the utility of autoradiography and cytopharmacology for drug targeting. Histochem Cell Biol 104:417–427
6. **Smith R, Stern G** 1967 Myopathy, osteomalacia and hyperparathyroidism. Brain 90:593–602
7. **Ritz E, Boland R, Kreusser W** 1980 Effects of vitamin D and parathyroid hormone on muscle: potential role in uremic myopathy. Am J Clin Nutr 33:1522–1529
8. **Simpson RU, Thomas GA, Arnold AJ** 1985 Identification of 1,25-dihydroxyvitamin D3 receptors and activities in muscle. J Biol Chem 260:8882–8891
9. **Costa EM, Blau HM, Feldman D** 1986 1,25-dihydroxyvitamin D3 receptors and hormonal responses in cloned human skeletal muscle cells. Endocrinology 119:2214–2220
10. **Zanello SB, Collins ED, Marinissen MJ, Norman AW, Boland RL** 1997 Vitamin D receptor expression in chicken muscle tissue and cultured myoblasts. Horm Metab Res 29:231–236
11. **Yoshizawa T, Handa Y, Uematsu Y, Takeda S, Sekine K, Yoshihara Y, Kawakami T, Arioka K, Sato H, Uchiyama Y, Masushige S, Fukamizu A, Matsumoto T, Kato S** 1997 Mice lacking the vitamin D receptor exhibit impaired bone formation, uterine hypoplasia and growth retardation after weaning. Nat Genet 16:391–396
12. **Weintraub H** 1993 The MyoD family and myogenesis: redundancy, networks, and thresholds. Cell 75:1241–1244

13. **Marlow SA, Kay PH, Papadimitriou JM** 1994 Polymorphism of the mouse transcription factor-encoding gene E2A. Gene 141:303–304
14. **Whalen RG, Sell SM, Butler-Browne GS, Schwartz K, Bouveret P, Pinset-Harstom I** 1981 Three myosin heavy-chain isozymes appear sequentially in rat muscle development. Nature 292:805–809
15. **Ezura Y, Tournay O, Nifuji A, Noda M** 1997 Identification of a novel suppressive vitamin D response sequence in the 5′-flanking region of the murine Id1 gene. J Biol Chem 272:29865–29872
16. **Pleasure D, Wyszynski B, Sumner A, Schotland D, Feldman B, Nugent N, Hitz K, Goodman DB** 1979 Skeletal muscle calcium metabolism and contractile force in vitamin D-deficient chicks. J Clin Invest 64:1157–1167
17. **Baczynski R, Massry SG, Magott M, el-Belbessi S, Kohan R, Brautbar N** 1985 Effect of parathyroid hormone on energy metabolism of skeletal muscle. Kidney Int 28:722–727
18. **Garber AJ** 1983 Effects of parathyroid hormone on skeletal muscle protein and amino acid metabolism in the rat. J Clin Invest 71:1806–1821
19. **Rescan PY** 2001 Regulation and functions of myogenic regulatory factors in lower vertebrates. Comp Biochem Physiol B Biochem Mol Biol 130:1–12
20. **Hughes SM, Cho M, Karsch-Mizrachi I, Travis M, Silberstein L, Leinwand LA, Blau HM** 1993 Three slow myosin heavy chains sequentially expressed in developing mammalian skeletal muscle. Dev Biol 158:183–199
21. **Wheeler MT, Snyder EC, Patterson MN, Swoap SJ** 1999 An E-box within the MHC IIB gene is bound by MyoD and is required for gene expression in fast muscle. Am J Physiol 276:C1069–C1078
22. **Swoap SJ** 1998 In vivo analysis of the myosin heavy chain IIB promoter region. Am J Physiol 274:C681–C687
23. **Allen DL, Sartorius CA, Sycuro LK, Leinwand LA** 2001 Different pathways regulate expression of the skeletal myosin heavy chain genes. J Biol Chem 276:43524–43533
24. **Gundersen K, Rabben I, Klocke BJ, Merlie JP** 1995 Over-expression of myogenin in muscles of transgenic mice: interaction with Id-1, negative cross regulation of myogenic factors, and induction of extra synaptic acetylcholine receptor expression. Mol Cell Biol 15:7127–7134
25. **Buckingham M, Houzelstein D, Lyons G, Ontell M, Ott MO, Sassoon D** 1992 Expression of muscle genes in the mouse embryo. Symp Soc Exp Biol 46: 203–217
26. **Seoane S, Alonso M, Segura C, Perez-Fernandez R** 2002 Localization of a negative vitamin D response sequence in the human growth hormone gene. Biochem Biophys Res Commun 292:250–255
27. **Nishishita T, Okazaki T, Ishikawa T, Igarashi T, Hata K, Ogata E, Fujita T** 1998 A negative vitamin D response DNA element in the human parathyroid hormone-related peptide gene binds to vitamin D receptor along with Ku antigen to mediate negative gene regulation by vitamin D. J Biol Chem 273: 10901–10907
28. **Sakoda K, Fujiwara M, Arai S, Suzuki A, Nishikawa J, Imagawa M, Nishihara T** 1996 Isolation of a genomic DNA fragment having negative vitamin D response element. Biochem Biophys Res Commun 219:31–35
29. **Bischoff HA, Stahelin HB, Dick W, Akos R, Knecht M, Salis C, Nebiker M, Theiler R, Pfeifer M, Begerow B, Lew RA, Conzelmann M** 2003 Effects of vitamin D and calcium supplementation on falls: a randomized controlled trial. J Bone Miner Res 18:343–351
30. **Janssen HC, Samson MM, Verhaar HJ** 2002 Vitamin D deficiency, muscle function, and falls in elderly people. Am J Clin Nutr 75:611–615
31. **Larsen ER, Mosekilde L, Foldspang A** 2001 Determinants of acceptance of a community-based program for the prevention of falls and fractures among the elderly. Prev Med 33:115–119
32. **Verhaar HJ, Samson MM, Jansen PA, de Vreede PL, Manten JW, Duursma SA** 2000 Muscle strength, functional mobility and vitamin D in older women. Aging (Milano) 12:455–460
33. **Pfeifer M, Begerow B, Minne HW** 2002 Vitamin D and muscle function. Osteoporos Int 13:187–194
34. **Talmadge RJ** 2000 Myosin heavy chain isoform expression following reduced neuromuscular activity: potential regulatory mechanisms. Muscle Nerve 23: 661–679
35. **Goldspink G, Scutt A, Loughna PT, Wells DJ, Jaenicke T, Gerlach GF** 1992 Gene expression in skeletal muscle in response to stretch and force generation. Am J Physiol 262:R356–R363
36. **Kischel P, Stevens L, Montel V, Picquet F, Mounier Y** 2001 Plasticity of monkey triceps muscle fibers in microgravity conditions. J Appl Physiol 90: 1825–1832
37. **Picquet F, Stevens L, Butler-Browne GS, Mounier Y** 1998 Differential effects of a six-day immobilization on newborn rat soleus muscles at two developmental stages. J Muscle Res Cell Motil 19:743–755
38. **Witzemann V, Sakmann B** 1991 Differential regulation of MyoD and myogenin mRNA levels by nerve induced muscle activity. FEBS Lett 282:259–264

0013-7227/02/$15.00/0
Printed in U.S.A.

The Journal of Clinical Endocrinology & Metabolism 87(4):1791–1796

Association between AAAG Repeat Polymorphism in the P3 Promoter of the Human Parathyroid Hormone (PTH)/PTH-Related Peptide Receptor Gene and Adult Height, Urinary Pyridinoline Excretion, and Promoter Activity

MASANORI MINAGAWA, TOSHIYUKI YASUDA, TOMOYUKI WATANABE, KANSHI MINAMITANI, YOSHIHITO TAKAHASHI, DAVID GOLTZMAN, JOHN H. WHITE, GEOFFREY N. HENDY, AND YOICHI KOHNO

Department of Pediatrics, Chiba University Graduate School of Medicine (M.M., T.Y., T.W., K.M., Y.T., Y.K.), Inohana, Chuo-ku, Chiba 260-8670, Japan; Department of Pediatrics, National Chiba Hospital (T.Y.), Tsubakimori, Chuo-ku, Chiba 260-8606, Japan; Departments of Physiology and Medicine (D.G., J.H.W., G.N.H.) and Human Genetics (G.N.H.), McGill University, Montréal, Québec, Canada H3G 1Y6; and Calcium Research Laboratory, McGill University, Royal Victoria Hospital (D.G., G.N.H.), Montréal, Québec, Canada H3A 1A1

The PTH/PTHrP receptor (PTHR1) plays an essential role in skeletal development and mediates many other functions of PTH and PTHrP. Human PTHR1 gene transcription is controlled by three promoters, P1–P3. The most proximal promoter, P3, is active in bone and osteoblast-like cell lines and accounts for the majority of renal transcripts in adults. We have identified a tetranucleotide repeat (AAAG)n polymorphism in the P3 promoter. In 214 unrelated Japanese, the repeat number (n) ranged from 3–8, with the AAAG5 allele being the most frequent (59%). In 55 unrelated Caucasians, n ranged from 5–7, and the frequency of the AAAG5 allele was 78%. The most frequent genotypes in a cohort of 85 young (18–20 yr) female Japanese were 5/5, 5/6, and 6/6. The 6/6 genotype was associated with greater height (5/5 *vs.* 6/6; $P < 0.02$) and lower urinary deoxypyridinoline and pyridinoline ($P < 0.02$), which are markers of bone resorption. The height of an additional 71 healthy female Japanese subjects, aged 14–17 yr, having genotype 5/5, 5/6, or 6/6 was also in the order of genotype 5/5 < 5/6 < 6/6 (5/5 *vs.* 6/6, $P < 0.05$). There was no significant difference in lumbar and femoral bone mineral density between genotypes. Likewise, there was no difference in circulating intact PTH levels between groups. The activity of P3 promoter-luciferase reporter constructs in transcription assays in 2 human osteoblast-like cell-lines varied according to repeat number, with AAAG6 being the least active. In conclusion, the P3 promoter (AAAG)n polymorphism is frequent in both Japanese and Caucasians and has potential as a linkage marker for the PTHR1 locus. In addition, it may influence the expression of the receptor in target tissues and have functional consequences on the developing skeleton. (*J Clin Endocrinol Metab* 87: 1791–1796, 2002)

PTH AND THE hormonally active metabolite of vitamin D, 1,25-dihydroxyvitamin D, are the principal regulators of calcium homeostasis. PTH exerts its calciotropic effects by acting on target tissues, bone and kidney (1). The PTHrP, originally discovered as the cause of hypercalcemia of malignancy, is a second member of the PTH family (2). PTHrP acts in many tissues as an autocrine/paracrine factor to regulate both cell proliferation and differentiation. In the bone growth plate, PTHrP regulates the differentiation of prehypertrophic chondrocytes into hypertrophic chondrocytes and inhibits their apoptosis, which precedes bone synthesis in the process of endochondral bone formation (3).

The actions of both PTH and PTHrP are mediated through the PTH/PTHrP receptor (PTHR1) with similar efficacy (4). This receptor belongs to the vast family of G protein-coupled receptors containing seven transmembrane domains. Binding of ligand(s) can stimulate the production of intracellular cAMP and IP3 (5).

We have cloned and characterized well conserved promoters (P1 and P2) of the mouse and human PTHR1 gene (6–8) and, more recently, have identified and characterized a third promoter, P3, that is highly expressed in the human, but not in the mouse (9). The human P3 promoter is (G+C) rich and contains Sp1 consensus binding sequences as well as an A-rich sequence. The P3 promoter in the human PTHR1 gene is the main promoter in kidney and bone (9).

Recently, we have identified an (AAAG)n polymorphism in the P3 promoter region of the PTHR1 gene (10). As the PTHR1 plays major roles in mediating both endocrine PTH actions in bone and kidney and also the paracrine/autocrine PTHrP action in endochondral bone growth (2), we examined the frequency of this polymorphism and its relation to adult height, bone mineral density (BMD), bone resorption markers, and PTH levels in a Japanese population. We found that this polymorphism is prevalent in both Japanese and Caucasians and that there are significant relationships between adult height and bone resorption markers and the repeat number.

Subjects and Methods

Subjects

Eighty-five healthy Japanese women, aged 18–20 yr (height SD score, −2.2 to +2.4; body mass index, 18.4–27.3), were recruited (group A). All of them had regular menses and undertook normal physical activity.

Abbreviations: BLC, Blomstrand lethal chondrodysplasia; BMD, bone mineral density; PTHR1, PTH/PTHrP receptor.

After overnight fasting, blood was drawn between 0700–0800 h for measurement of biochemical parameters and DNA isolation, and the second voided morning urine was collected. Lumbar and femoral neck BMDs were measured by dual energy x-ray absorptiometry using QDR-1000 (Hologic, Inc., Waltham, MA) as previously described (11). Genomic DNA was also obtained from 129 healthy Japanese (group B) and 55 normal Caucasians (group C) for analysis of the PTHR1 gene polymorphism. Among group B, we analyzed height in 71 healthy female subjects, aged 14–17 yr, with genotypes 5/5, 5/6, and 6/6. Informed consent was obtained from each participant.

Biochemical parameters

In group A, we measured serum PTH, urinary deoxypyridinoline, and pyridinoline as markers for parathyroid function and bone resorption, respectively, and we also measured serum calcium, phosphorus, alkaline phosphatase, and 1,25-dihydroxyvitamin D. Serum PTH was measured in two assays by a midregion-specific RIA (High Sensitive PTH, Yamasa Shoyu Co. Ltd., Chiba, Japan) and an immunoradiometric assay (Intact PTH, Nichols Institute Diagnostics, San Juan, CA). Urinary deoxypyridinoline and pyridinoline were measured by HPLC and were expressed as a ratio of urinary creatinine (deoxypyridinoline/creatinine, pyridinoline/creatinine; nanomoles per mmol). Serum calcium and phosphorus were measured colorimetrically in a Hitachi 764 autoanalyzer (Hialeah, FL).

DNA isolation and PCR amplification

DNA was isolated from peripheral blood using standard procedures, and nested PCR was employed for amplification of the minimal region of the P3 promoter including the A-rich region (Fig. 1A). PCR was performed using 20 ng genomic DNA or 0.4 μl of the first PCR product, 15 pmol of each primer, 200 μmol/liter dNTPs, 1.5 mmol/liter $MgCl_2$, 4% dimethylsulfoxide, 1 × Expand HF buffer, and 1 U enzyme mix of the Expand High Fidelity PCR System (Roche Molecular Biochemicals, Tokyo, Japan) in a total volume of 20 μl. The sequences of the forward primer and reverse primer for the first PCR are: P3(−254), 5′-AATAACAGGTTCCTGCGCGC-3′; and P3R(+205), 5′-GGGTGCAGAGCTGCGTCAGG-3′, respectively. Samples were cycled at 95 C for 50 sec, 65 C for 1 min, and 72 C for 1 min for 15 cycles, and then at 95 C for 50 sec, 63 C for 1 min, and 72 C for 1 min and 15 sec for 25 cycles, followed by 10 min at 72 C. The sequences of the forward primer and reverse primer for the second PCR are: P3(−175), 5′-GAAGCCACAGCTCCCATTTC-3′; and P3R(−34), 5′-TGCCTCGGAGCGAAGAAATC-3′, respectively. Samples were cycled at 95 C for 50 sec, 64 C for 30 sec, and 72 C for 20 sec for 40 cycles, followed by 6 min at 72 C. The final PCR products were separated on an 8% polyacrylamide gel (Fig. 1B) and were purified with a Qia-Quick gel extraction kit (QIAGEN, Hilden, Germany). Nucleotide sequencing was performed on several different samples from each individual using a model 373A automated sequencer (PE Applied Biosystems, Foster City, CA) with a *Taq* DyeDeoxy terminator cycle sequencing kit (PE Applied Biosystems) to confirm the AAAG repeat number.

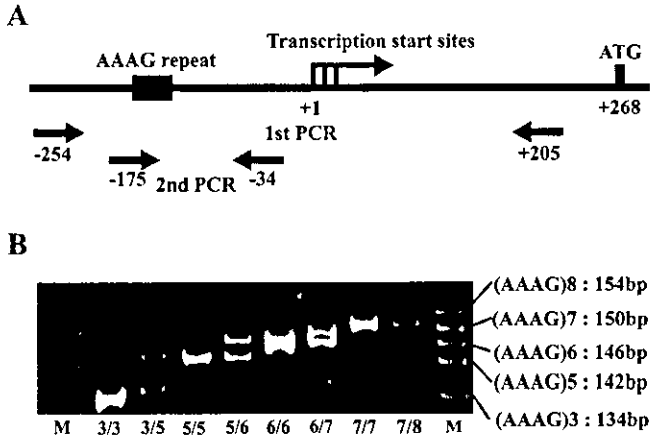

FIG. 1. PCR amplification of the region of the PTHR gene containing the AAAG repeat polymorphism. A, Promoter P3 of the PTHR gene and downstream sequence with the indicated positions of PCR primers. The positions of the AAAG repeat sequence, the transcription initiation start site (+1), and the ATG initiation codon (+268) are shown. B, Gel electrophoresis (8% polyacrylamide) of the products amplified by nested PCR from human genomic DNA. M, Markers, PCR products from eight different individual DNAs containing AAAG repeats 3–8. The genotypes of PCR products are indicated.

Construction of PTHR promoter-luciferase reporter vectors and transient transfection

The sequences of the forward primer and reverse primer of the PCR are P3(−181), 5′-CGCGGATCCTGGGGCGAAGCCACAGCTCC-3′ and P3R(+205), 5′-GCTCTAGAGGGTGCAGAGCTGCGTCAGG-3′, respectively (*underlined* sequences represent restriction enzyme sites added to facilitate subcloning). The PCR conditions were as described above. Samples were cycled at 95 C for 50 sec, 69 C for 1 min, and 72 C for 1 min for 15 cycles, and then at 95 C for 50 sec, 67 C for 1 min, and 72 C for 1 min 15 sec for 25 cycles, followed by 10 min at 72 C. PCR products were subcloned into the pBluescript SK^- plasmid and sequenced [T7 sequencing kit (Pharmacia Biotech, Uppsala, Sweden)]. The PCR fragments that included different (AAAG)n repeats (where n = 3, 5, 6, 7, or 8) were inserted into the polylinker of the luciferase reporter plasmid pXP2 (9). Human osteosarcoma SaOS2 and HOS cell lines were propagated in DMEM (Life Technologies, Inc., Tokyo, Japan) in 10% FBS (Life Technologies, Inc.). Cells were seeded in six-well plates at approximately 35% confluence, and the next day transfections were performed with Effectene Transfection Reagent (QIAGEN, Tokyo, Japan) using 0.6 μg luciferase reporter plasmid DNA and 0.2 μg β-galactosidase expression vector P610AZ. Cells were harvested 48 h later, and extracts were prepared by lysing cells in 250 μl reporter lysis buffer (Promega Corp., Tokyo, Japan), of which 50 μl were used for both β-galactosidase assay (for normalization of transfection efficiency) and luciferase assay (Promega Corp.). Results are the mean ± SEM of three independent experiments.

Statistical analysis

Statistical significance was determined by one-way ANOVA and Fisher's protected least significance difference using StatView J 4.02 software (Abacus Concepts, Inc., Berkeley, CA), and the data are presented as the mean ± SD unless otherwise noted.

Results

The (AAAG)n polymorphism in Japanese and Caucasian populations

In the Japanese population (groups A and B) the following allele frequencies were found: n = 3, 1.9%; n = 4, 0%; n = 5, 59.3%; n = 6, 36.2%; n = 7, 2.3%; and n = 8, 0.2%. The genotype frequencies were 3/3, 0.5%; 3/5, 1.9%; 3/6, 0.9%; 5/5, 35.0%; 5/6, 44.0%; 5/7, 2.8%; 6/6, 13.1%; 6/7, 1.4%; and 7/8, 0.5%, with a heterozygote frequency of 32.7%. In the Caucasian population (group C) the allele frequencies were: n = 5, 78.2%; n = 6, 20.0%; and n = 7, 1.8%. The genotype frequencies were: 5/5, 63.6%; 5/6, 29.1%; 6/6, 3.6%; and 6/7, 3.6%, with a heterozygote frequency of 59.5%. Thus, the AAAG5 is the most common in both populations and is more frequent in Caucasians.

Genotype, anthropometric characteristics, and serum biochemistries

The genotypes 5/5, 5/6, and 6/6 comprise 92% of Japanese individuals (see above). The genotypes, height, weight, and serum biochemistries of group A subjects are shown in Table

TABLE 1. Genotype, anthropometrics, biochemistries, and BMD of studied subjects (mean ± SD)

Genotype	Height (cm)	Weight (kg)	Serum calcium (mmol/liter)	Serum phosphorus (mmol/liter)	Serum intact PTH (ng/liter)	Serum mid-region PTH (ng/liter)	Serum $1,25(OH)_2D$ (ng/liter)	Serum ALP (IU/liter)	Urine deoxypyridinolline (nmol/mmol Cre)	Urine pyridinolline (nmol/mmol Cre)	Lumbar BMD (g/cm^2)	Femoral-neck BMD (g/cm^2)
5/5 (35)	157.3 ± 4.90	53.8 + 1.224	2.22 ± 0.07	1.28 ± 0.11	22.5 ± 9.2	189 ± 112	53 ± 14	126 ± 28	10.9 ± 2.7 (n = 29)	41.9 ± 8.1 (n = 29)	1.008 ± 0.105	0.958 ± 0.118
5/6 (32)	158.4 ± 4.49	52.1 + 1.023	2.20 ± 0.06	1.29 ± 0.12	26.9 ± 16.1	246 ± 118	53 ± 10	115 ± 34	11.0 ± 2.4 (n = 27)	40.1 ± 7.8 (n = 27)	1.010 ± 0.097	0.964 ± 0.094
6/6 (10)	161.6 ± 3.86[a]	53.0 + 0.596	2.20 ± 0.06	1.38 ± 0.33	23.1 ± 8.7	259 ± 113[b]	47 ± 12	121 ± 15	8.3 ± 2.4 (n = 8)[a]	29.7 ± 5.7 (n = 8)[a]	1.010 ± 0.127	0.982 ± 0.116

[a] Significantly different from the 5/5 genotype group ($P < 0.02$).
[b] Significantly different from the 5/5 genotype ($P < 0.05$).

1. Individuals of the 6/6 genotype were of significantly greater height (5/5 *vs.* 6/6, $P < 0.02$; Fig. 2A), whereas serum calcium, phosphate, intact PTH, 1,25-dihydroxyvitamin D, and alkaline phosphatase levels were not different between groups (Table 1). However, genotype 6/6 individuals had significantly higher circulating midregion PTH levels (5/5 *vs.* 6/6, $P < 0.05$). The height in 71 female subjects, aged 14–17 yr, in group B was 5/5 < 5/6 < 6/6 (5/5 *vs.* 6/6, $P < 0.05$; Fig. 2B). The height in group A did not correlate with biochemical parameters (PTH, urinary pyridinoline and deoxypyridinoline).

Genotype, markers of bone resorption, and bone density

Individuals with the 6/6 genotype excreted significantly lower concentrations of the bone resorption markers deoxypyridinoline and pyridinoline than those with 5/5 and 5/6 genotypes (Table 1 and Fig. 3). However, there was no significant difference in either lumbar spine or femoral neck

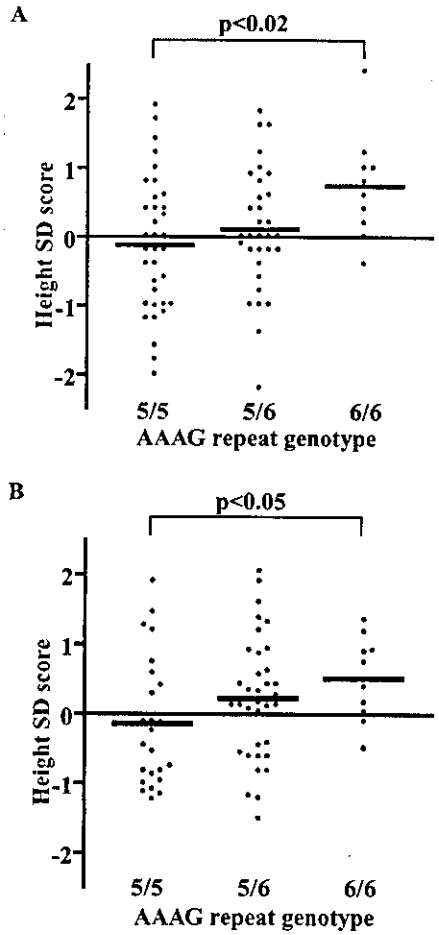

FIG. 2. A, Comparison of (AAAG)n polymorphism genotype and adult height (group A). Subjects were genotyped as described in *Subjects and Methods*. Mean height ± SD: 5/5, 157.3 ± 4.90 cm; 5/6, 158.4 ± 4.49 cm; and 6/6, 161.6 ± 3.86 cm. B, Comparison of (AAAG)n polymorphism genotype and height in 70 female subjects, aged 14–17 yr, in group B with genotypes 5/5, 5/6, and 6/6. There was a significant difference in height between genotypes 5/5 and 6/6 (B; $P < 0.05$).

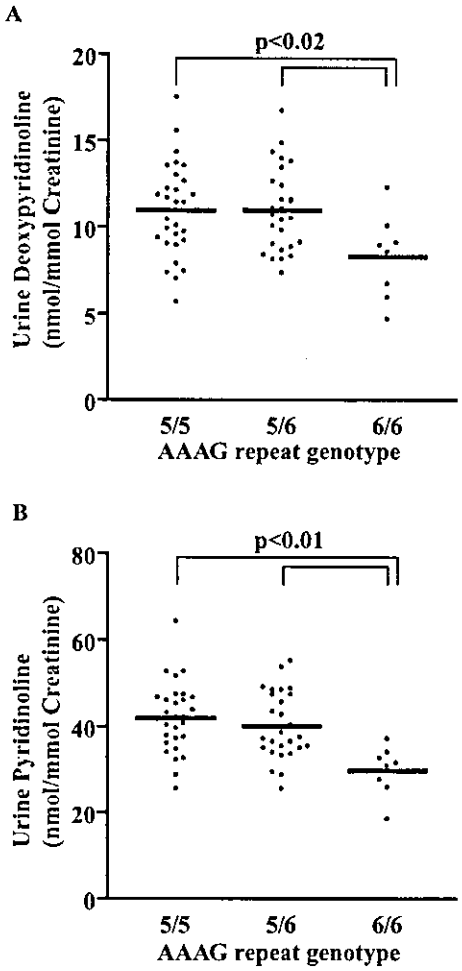

FIG. 3. Comparison of (AAAG)n polymorphism genotype and biochemical markers of bone resorption. A, Urinary deoxypyridinoline (nanomoles per mmol creatinine, mean ± SD): 5/5, 10.95 ± 2.71; 5/6, 10.96 ± 2.41; and 6/6, 8.29 ± 2.44. B, Urinary pyridinoline (nanomoles per mmol Cre; mean ± SD): 5/5, 41.93 ± 8.06; 5/6, 40.08 ± 7.81; and 6/6, 29.68 ± 5.67.

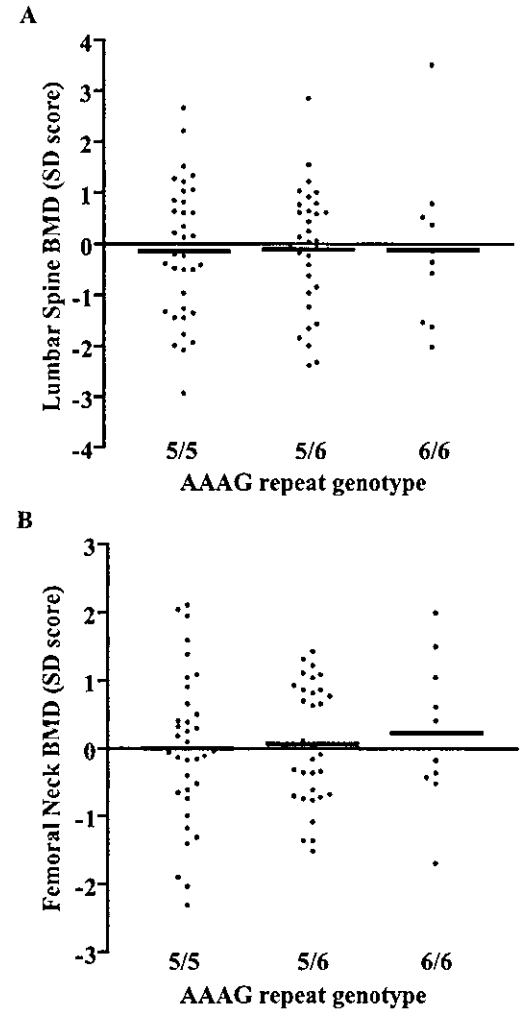

FIG. 4. Comparison of (AAAG)n polymorphism genotype and lumbar spine BMD and femoral neck BMD. A, Lumbar spine BMD: 5/5, 1.008 ± 0.105 g/cm^2; 5/6, 1.010 ± 0.097 g/cm^2; and 6/6, 1.010 ± 0.127 g/cm^2. B, Femoral neck BMD: 5/5, 0.958 ± 0.118 g/cm^2; 5/6, 0.964 ± 0.094 g/cm^2; and 6/6, 0.982 ± 0.116 g/cm^2. There were no significant differences in lumbar spine (A) and femoral neck (B) BMD between genotypes (see also Table 1).

BMD shortly after achieving peak bone mass between genotypes (Fig. 4).

Effect of AAAG repeat number on PTHR P3 promoter activity in vitro

The activities of PTHR1 P3 promoter-luciferase constructs representing all identified polymorphic variants were analyzed by transiently transfecting recombinants into human osteoblast-like SaOS-2 and HOS cell lines. Significant differences were observed in promoter activity between various constructs (Fig. 5) demonstrating that the AAAG repeat number influences the P3 promoter activity. Promoter activity was inversely related to repeat numbers from 3–6, and an increase in transcriptional activity was noted for AAAG8.

Discussion

The P3 promoter in the human PTHR1 gene is active in target tissues, bone and kidney. In the present study we identified a tetranucleotide repeat (AAAG)n polymorphism in this promoter region in both Japanese and Caucasians, with the AAAG5 allele being the most frequent in both. The 5/6 genotype comprises 44% of Japanese subjects and is predominant, whereas the genotype 5/5 accounts for 64% of Caucasians. Thus, this polymorphism is frequent, and it could be a useful tool in linkage analysis of quantitative traits to the PTHR1 locus.

Our previous studies have shown that the AAAG repeat region represses P3 promoter activation in gene transfer experiments performed in human osteoblast-like SaOS-2 and HOS cells (12). In the present study the functionality of the expansion and contraction of the AAAG repeat number was demonstrated *in vitro* by transfecting P3 promoter/reporter constructs into SaOS-2 and HOS cells. Promoter function varied according to repeat number, with the AAAG6 variant exhibiting the least activity. If this finding is reflected by the